UNIVERSITY OF TARTU
FACULTY OF SCIENCE AND TECHNOLOGY
Innovation and Technology Management Curriculum

Hilary Somtochukwu Emenike

Exploiting Human-emitted Thermal Radiation

Master Thesis (30 EAP)

Supervisor: Huber Flores

TARTU, 2021

Abstract

Waste is a growing concern for global sustainability, affecting everything from economic development to human health. Effective waste management is critical for mitigating the harmful effects of waste accumulation on society. In this thesis, we develop MIDAS, an innovative sensing approach for effective household waste management. MIDAS builds on the fact that people need to touch objects when they are throwing them away and that these interactions result in thermal footprints on the objects' surface. By examining the dissipation of the respective thermal footprints, it is possible to identify the waste material and support effective sorting and recycling practices. We validate our approach through extensive empirical benchmarks, demonstrating that MIDAS can recognize a wide range of materials and generalize variations in the people interacting with objects. Our solution paves towards improved sustainability by offering an innovative solution for classifying materials and optimizing household waste management practices.

CERCS: P170 Computer science, numerical analysis, systems, control

Keywords: thermal imaging, waste management, mobile computing, pervasive computing, recycling solutions, IoT

Inimesest eraldunud soojusliku kiirguse kasutamine

kokkuvõte: Jäätmed on kasvav probleem globaalsele jätkusuutlikkusele, mõjutades kõike alates majanduslikust arengust kuni inimeste terviseni. Tõhus jäätmekäitlus on väga oluline kahjulike jäätmete mõjude leevendamiseks ühiskonnas. Selles magistritöös arendame MIDAS, mis on innovatiivne lähenemisviis majapidamisjäätmete tõhusale käitlemisele. MIDAS tugineb faktile, et inimesed peavad objekte puutuma, enne kui need ära visatakse ning

nende tegevuste koosmõjude tagajärjel tekivad esemetele soojuslikud jäljed. Uurides vastavate soojuslike jälgede hajumist, on võimalik kindlaks teha jäätme materjal ning toetada tõhusaid sorteerimis- ning taaskasutusharjumusi. Me kinnitame lähenemisviisi läbi ulatuslike võrdlusaluste, näidates, kuidas MIDAS suudab kindlaks teha ulatuslikku valikut erinevaid materjale ning tuvastada muutuseid, kui inimesed objekte puudutavad. Meie lahendus aitab saavutada jätkusuutlikkust, pakkudes materjalide tuvastamiseks uudset lahendust ja majapidamisjäätmete käitlemisele parimat lahendust leida.

CERCS: P170 Arvutiteadus, arvutusmeetodid, süsteemid, juhtimine

Märksõnad: termopildistamine, jäätmekäitlus, mobiilne andmetöötlus, kõikehõlmav andmetöötlus, ringlussevõtu lahendused, IoT

Contents

List of Figures

LIST OF FIGURES

List of Tables

Acknowledgements

Firstly, big thanks to family and friends without whom I would not have written this work. I would also like to acknowledge Prof. Dr. Huber Flores for his numerous helpful suggestions, guidance, encouragement, and enthusiasm during the project. Next, special gratitude goes out to Farooq Dar and Mohan Liyanage for their assistance during the experiment; their help was crucial for completing this work. Finally, huge thanks to all participants who took part in the experiments; there will be no MIDAS without you.

1

Introduction

Accumulation of waste is a growing concern for global sustainability, with both the volume and complexity of waste are increasing every year. According to a report by the World Bank, an estimated 2.01 billion tonnes of waste is produced each year, which contributes to approximately 5% of annual greenhouse gas emissions (3). Besides affecting climate, waste is detrimental to natural ecosystems (4) and affects flora and fauna, and even human health (5). Projections suggest that the amount of waste produced by a person in a single day will continue to grow, reaching an estimated 0.88 kg per person by 2050, which is a 19% increase from the current average of 0.74. kg per person (3). As these projections show, the amount of waste is not likely to decrease soon, making effective waste processing and management critical for counteracting its harmful effects. Waste management and recycling solutions are critical to overcome global concerns (6), such as pollution of natural ecosystems (4), climate change (5), and reduction rate of generated waste per person (7). Waste causes pollution that affects flora and fauna, and even human health (8). The main issue with waste is its incremental and accumulative generation over the years. Indeed, lands and underwater areas are filled with waste that decomposes over long periods of time (9), from decades to centuries-for instance, the great pacific garbage patch. More cumbersome, it is expected that by 2025, the generation of waste per person daily increases from 1.2 kg to 1.5 kg, which makes the problem of waste management very relevant. *Waste management* is critical for counteracting the harmful effects of waste accumulation and improving global sustainability. Internet of Things and emerging sensor technologies can potentially facilitate this process by assisting people in waste management decisions and

optimizing existing waste management processes (10). Currently, however, technological means for supporting waste management are limited, with the main approach being manual recycling and regulatory constraints (11). While recycling practices can mitigate negative concerns from waste accumulation, they are prone to human error and provide only a coarse categorization of waste and waste production (12). The best practices also need to educate the citizens, public awareness on environmental education by promoting a positive attitude towards the environment. Although there are some previous efforts on using IoT and sensor technologies, e.g., using cameras or other sensor modalities, during waste sorting or as part of the trash bins (13), the adoption of these techniques has remained low due to the need for specialized hardware or operating conditions (e.g. unobstructed view of objects). These solutions also fail as they can only be applied late during the waste management chain, making reuse costly and limiting the usability (14, 15). As a result, many materials are unlikely to be reused, resulting in further waste accumulation. With the recent accumulation of used respiratory masks and other PPE (Personal protective equipment) equipment becoming a significant waste concern (16).

We aim to exploit the capability of state-of-the-art technique, thermal sensing, which is an emerging technology that measures object reflectivity (17). To produce an image of it or locate the object, it utilizes heat generated from an object (18). Costs and size are declining as thermal cameras become more popular and cheaper, although efficiency and image resolution are increasing, opening up new application areas in recent years. Several studies have shown the reliability and usefulness of the thermal imaging technique (19, 20), with these cameras being reasonably simple to use and offering a quick way to detect defects in buildings (21, 22), pipeline irregularities (23), bridge deck delamination (24). It also allows data to be collected and an object to be analysed. Thermal cameras are robust, discrete, and easy to install (25).

In this thesis, we contribute by developing MIDAS as a novel sensing solution for categorizing household waste and supporting early prevention of disposed materials into mixed waste. MIDAS takes advantage of the fact that people need to touch objects when interacting with them. As a result of the human touching the item, the object's surface contains a thermal fingerprint, which dissipates over time, with the object's material affecting the rate of dissipation. MIDAS captures these effects using a thermal camera

and constructs a thermal dissipation fingerprint that can be used to categorize materials and support waste management. We validate MIDAS through rigorous benchmark experiments that consider a wide range of materials. As part of the study, we also conduct a user study with 18 participants to demonstrate that MIDAS generalizes to human temperature variations. Our results indicate that human-emitted radiation can be used to characterize different object materials. To prove that MIDAS is not limited to supporting waste management, we also present an application of our technique for detecting abnormal human temperature for supporting health applications. MIDAS thus offers a novel sensing approach that is highly useful for optimizing waste management solutions and can also help a broader range of innovative applications.

1.1 Contributions

The following sums up the contributions:

- **Novel method:** We develop MIDAS as a novel sensing approach for characterizing materials using thermal dissipation footprints and demonstrate usefulness of MIDAS in household waste classification.
- **Novel insights:** We demonstrate that current state-of-the-art techniques based on computer vision are limited and only capable of recognizing products that are not mixed with other waste items. We also highlight the importance of analyzing objects at the level of material properties to increase robustness of results.
- **Improved performance:** We perform rigorous benchmarks demonstrating that MIDAS significantly improves the classification of waste materials of different sizes and shapes and works robustly across different persons.

1.2 Outline

This thesis is structured as follows:

- Chapter 2 reviews the state-of-the-art about infrared thermal imaging, its limitations as well as its application in computer systems. Moreover, we also demonstrate how existing sensing techniques based on automated computer vision and light-sensing fail in waste management systems.

- Chapter 3 describes the different types in which waste is classified and presents a feasibility analysis of material characterization using human-emitted thermal radiation.
- Chapter 4 describes the thermal imaging processing pipeline and methodology used in this thesis.
- Chapter 5 describes the experimental testbed designed to capture video footage of thermal footprints for different objects materials.
- Chapter 6 presents our findings
- Chapter 7 discusses the implications and limitations of our work
- Chapter 8 presents the summary and conclusion of our work

2

State of the Art

This chapter reviews thermal imaging, which is the groundwork of this thesis and presents an overview of recent research that we consider relevant for this study. We start by showing a background knowledge of the detection sensors, focusing on the thermal sensing technique and how it has been applied in computer systems. We then review previous knowledge on material sensing and waste management, and recycling systems through thermal imaging. We also demonstrate how existing sensing techniques that are based on automated computer vision (13, 26) and light-sensing (27) fail in categorizing waste, especially when the objects are mixed with other waste items. In our work, we attempt to overcome these limitations.

2.1 Passive sensing (IR Thermal imaging)

According to J. Fraden, "a sensor is a device that receives stimulus or an input signal and responds with an electrical signal bearing a known relationship to the input" (28). Sensors can be found in most electrical devices and are designed to support various applications, such as surveillance, tracking, monitoring, and mapping. Currently, there are two categories of sensors, active and passive sensors. An active sensor provides a source of light while also transmitting and detecting energy simultaneously. Conversely, passive sensors do not provide illumination to produce output signals and measure variations based on natural emission (29). Thermal imaging falls in this last category.

Infrared Thermal imaging, also known as Infrared thermography, is the recording and measurement of heat radiation using specialized cameras. These cameras work in an

environment without ambient light and can penetrate thick fog such as smoke and haze. The first Thermal cameras were initially developed for military purposes in the 1950s and 1960s and have since evolved, enabling applications that were impossible to do easily in the past due to the high cost of production and limited availability. Thermal cameras are similar to digital photographic cameras but record thermal infrared radiation (TIR). Infrared radiation is invisible to the human eye as it occurs beyond the red end of the visible light spectrum (Table 2.1 describes the different light spectrum). However, thermal radiation is located within the infrared range of the electromagnetic spectrum (30). The visible wavelength range from $0.4 - 0.78\mu m$ while infrared radiation has a longer wavelength, ranging from $0.78 - 1000\mu m$ (31); Thermal cameras operate in the infrared band of the electromagnetic spectrum with wavelengths between $2 - 14\mu m$. The infrared spectrum which is subdivided into near-infrared (NIR) $0.78 - 2.5\mu m$, mid-infrared (MIR) $1.3 - 8\mu m$ and far-infrared (FIR) $7.5\mu m$ and $13\mu m$ (32), and are used for monitoring temperatures of different range from -50 to 2000°C. All objects with a temperature above absolute zero (-273°C) emit infrared radiation, and not only objects we think of as warm emit infrared radiation (IR). Thermal imaging determines an image temperature based on the absolute temperature of the object (Figure 2.1 shows an example of this). The image is formed based on the object's heat signature and records the items' current signatures based on their heat pattern. During operation through image analysis, the thermal infrared camera heats-up, making it a thermal radiation source. They have an inbuilt thermometer and perform radiometric calibration at regular time intervals to make up for this. In the course of calibration, frames are lost because a plate of known temperature is inserted in front of the sensor during this process.

2.2 Thermal detection types

Thermal detection is a mechanism that changes some of a material's measurable properties due to the rise in temperature of that material caused by electromagnetic radiation absorption (17). The resistive bolometric effect, the pyroelectric effect, and its modification (known as either the bias enhanced pyroelectric effect or the ferroelectric bolometer) and the thermoelectric effect (17) are the most important. However, there

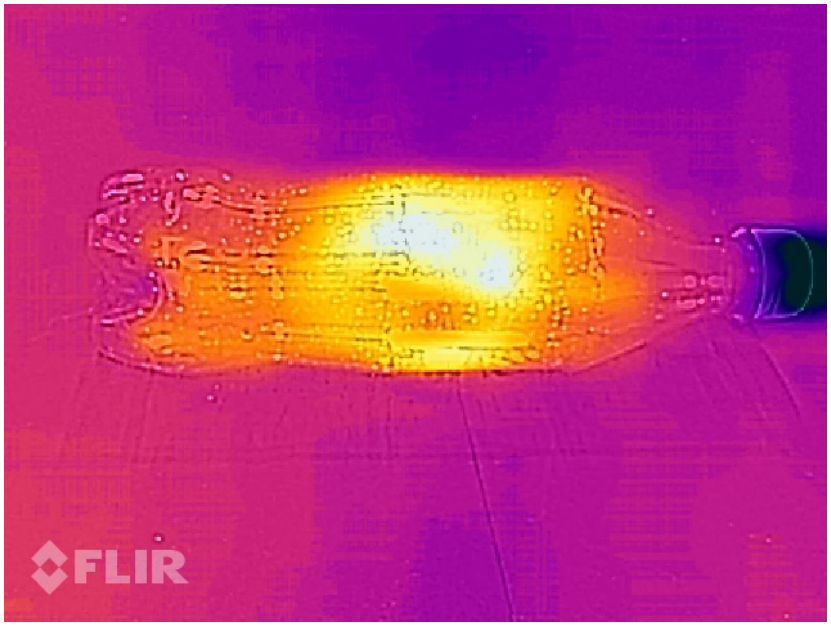

Figure 2.1: Example of a thermal image from a plastic bottle that is exposed to ambient heat.

Table 2.1: The electromagnetic spectrum(2)

Wave	**Wavelength (meters)**	**Frequency (Hz)**
AM Radio	10^{2}	10^{6}
FM, TV	1	10^{8}
Radar	10^{-2}	10^{9}
Infared	10^{-6}	10^{13}
Visible Light	10^{-7}	10^{15}
Ultraviolent (UV)	10^{-8}	10^{16}
X-Rays	10^{-10}	10^{18}
Gamma Rays	10^{-14}	10^{21}

are several thermal detection mechanisms. Uncooled thermal detectors have been developed primarily with thermal and ferroelectric microbolometer detectors (using Barium Strontium Titanate (BST) as detector material, which suffers from halo effect) (33). Due to their advantages over ferroelectric detectors, microbolometers have the most significant market share.

2.3 Advantages and limitations of thermal imaging

Although thermal cameras cannot perform person identification in contrast to visible light cameras, it is both an advantage and a limitation. When preserving the individual's identification is paramount, thermal cameras can be used in such situations. However, if the individual's identity is requested, it must be integrated with a visible light camera. Furthermore, thermal cameras are favored over visual cameras in most outdoor situations. They record a very high performance where there is temperature difference associated in object to be detected, such as emerging fire, integrated night vision thermal camera to see human activities or motion in cross border checkpoints, increased or abnormal body temperature differences in heat transfer in materials. This is because thermal cameras are sensitive to emitted radiation and produce an image with little or no distortions at night or harsh weather conditions such as snow, rain, or fog. Regarding temperature measurements, thermal cameras are useful when measuring the temperature over a large area compared to point-based methods. However, the accuracy of temperature measurement is considered not as accurate as contact methods. Finally, a key limitation of existing imaging techniques is that they focus on external characteristics of reflection or absorption, which are dependent on the shape, color, and other properties of the items rather than capturing only intrinsic characteristics of the materials themselves. Thermal images cannot be captured through certain materials like water and glass. These materials are highly reflective in the thermal spectrum as opaque, which is a significant disadvantage for situations where individuals' images in cars need to be captured.

2.4 Application in computer systems

With thermal imaging becoming popular, this section briefly discusses thermography as a useful technology in different fields. This detection technique is used in computer systems, which uses sophisticated image analysis algorithms and a computer to reconstruct the images to show heat patterns.

2.4.1 Medical thermography

Computer systems are used for image processing and monitoring of thermal radiation changes. In a medical analysis, thermography based computer-assisted detection/diagnosis (CAD) systems help to screen for fever patients in places with a high volume of people, such as airports and border crossings (34, 35). The early detection of the diabetic foot, specifically, CAD systems for diabetic foot (36), help prevent complications and amputation. They have also been shown to reveal tumors in an early stage, most notably breast cancer (37). Medical issues such as the behavior of ciliary muscle of the human eye (38), the periodic fluctuation in skin temperature (39) or the measuring of blood flow rate in superficial veins (40), can be studied from thermal images.

2.4.2 Facial analysis

An individual's face is a biometric trait that can be applied in an automated computer-based security system for authentication purposes. Experts are investigating and developing methods for the improvement of face recognition (41). Humans' stress levels can be detected using thermal imaging based on their face's heat radiation. The thermal facial analysis was used for deception detection (42). Pavlidis et al. (43) also proposed this technique to capture anxiety.

2.4.3 Fire detection and military

With firefighters' inability to see through smoke quickly, they can be robbed of their most essential commodities (sight) when they fight fires and, as such, handicapping their ability to perform effectively, find the hot spot, and locate victims. Identification of objects that could pose a risk is of great importance. A fire detection system can be used for mobile robots (44) by locating the hot spots, the robot is directed to the fire source. Arrue et al. (45) proposed an alternative real-time infrared-visual system for forest fire detection, composed of both thermal and visual cameras and meteorological and geographical information. In the military, Price et al. (46) presented the Gunfire Detection and Location (GDL) system for military applications to detect gunfire. Gunfire is detected in Mid-Wave IR (MWIR) imager and validated by acoustic events.

2.4.4 Aerial thermography

With UAV (Unmanned aerial vehicle) becoming more popular and improving in sophistication and reliability, various studies have investigated methods of using drones for problem-solving, be it in the delivery service industry (47), video surveillance (48), rescue(49), which can perform the mission with increasing levels of complexity which is sometimes considered dangerous by humans. Thermal sensors have been integrated into some UAVs for tracking and monitoring the behavior of certain physical property and temperature changes over time. Remote sensing in Unmanned aerial vehicle (UAV) which aids data collection has developed rapidly from a researching stage to a more practical approach, which is applied in various fields (50). The authors in (51), used aerial thermography to perform dense crowd detection effectively. They proposed region of interest (ROI) extraction and a two-stage blob based approach for pedestrian detection, by first extracting pedestrian blobs using the regional gradient feature and geometric constraints. The detected blobs are classified utilizing Support vector machine (SVM) technique with a hybrid descriptor. Furthermore, in archaeology, UAVs collect aerial imagery from specific altitudes at different weather conditions at any given time. J. Casana et al. (52) propose aerial thermography to detect archaeological sites. The camera was sensitive to 0.05°C temperature increments and recorded 640 by 512 pixel video at 8-bit radiometric resolution. Pedestrian survey and subsurface testing were carried out, which was proceeded by aerial imaging to detect surface and subterranean features not immediately visible from ground level. The thermal imagery was consistently successful at detecting nearly all archaeological features that were previously recorded through Pedestrian survey and subsurface testing, where other remote sensing techniques had failed repeatedly.

2.5 Material sensing

Materials have different characteristics of different properties, which can be exploited to categorize them. Examples include the use of variations in WiFi signal propagation characteristics to identify liquids (53), and the use of surface tension to characterize liquids (54, 55). The most common material sensing approach relies on different light spectrum parts and measures either reflection or absorption at different frequencies. Examples range from the use of green light sensing to detect plastic waste (56) to the

use of near-infrared sensing to facilitate medicine adherence (57) and the use of hyperspectral imaging for estimating sugar content in drinks (58). Also, deep learning approaches for detecting different material types from reflection patterns at different wavelengths have been proposed (59). Other works have used smartphone cameras to analyze liquids' (54, 55), identifying objects via material reflection (60), and to learn the quality of food using RFID (Radio-frequency identification) stickers (61). These methods operate by transmitting light at near-infrared frequencies ($780 - 2500nm$) through the production and measuring absorption properties at the different wavelengths (62). In spectroscopy, Near-infrared sensing was also used to facilitate medicine management in elderly care (57). Green light-sensing has also been used to characterize waste underwater (56). Our work extends these works by using infrared spectrum to estimate internal characteristics of materials related to heat dissipation.

2.6 Waste management and recycling systems

The most common IoT-based approach for waste management is to use computer vision (13, 26). Several sensor-based systems exist to detect, sort accurately, and separate the waste (63, 64, 65). Other methods, such as hyperspectral based sorting (HSI) (66), and spectroscopic analysis (67) also have been proposed. IoT was also seen in combination with infrared sensing to communicate to waste managers (27). Gundupalli et al. used thermal imaging technique for the classification of dry recyclables (68), obtained from municipal solid waste (MSW) in recycling plants. Randomly selected MSW was kept in a hot dark chamber and heated up to generate radiation. They obtained a classification success rate in the range of 85–96 percent for various materials. Classification of metallic fractions (MFs) and non-metallic particles (NMFs) of e-waste using thermal imaging-based technique operated in the long-wave infrared range (LWIR, $8 - 15\mu m$) was also proposed in recent literature (69). They obtained a classification success rate in the range of 84–96 percent. In contrast to the prior literature, we study the early identification of waste material by piggybacking the human-emitted thermal radiation. Our approach aims to classify waste before it gets mixed with others, such that the separation of waste for recycling becomes less problematic.

2.7 Existing approaches for waste detection (Baselines)

In this section, we demonstrate how existing sensing techniques based on automated computer vision (13, 26) and light sensing (27) fail in categorizing waste, especially when the objects are mixed with other waste items.

2.7.1 Computer vision analysis

Experiment: We first attempt to classify household waste using computer vision and train a state-of-the-art Convolutional Neural Networks (CNNs) model using the publicly available TrashNet dataset (70). We focus exclusively on the plastics category which contains 626 images of plastic waste for training the deep learning model. The dataset has images where the individual pieces are shown against a white background. As such images do not match realistic recognition settings, we supplement the dataset with an additional 767 images from the Japan Agency for Marine Earth Science and Technology (JAMSTEC) Deep-sea Debris Database dataset.

Collected images were annotated manually by drawing a rectangle box around the waste material in images. We labeled the TrashNet plastic items as "trash" and the JAMSTEC plastic items as "plastic". Both datasets were augmented by adding noise, hue, blue, horizontal flip, and vertical flip modifications to each original image, resulting in a total of 6985 for model training input. We created and trained the PlasticNet model using Google Collab server GPU, with 100k iterations and a batch size of 12, running TensorFlow Lite 1.15. For the base training model, ssd_mobilenetv2_oidv4 was used.

Results: For validation, we used 31 images depicting real tossed plastic waste (1). In total, 33 separate waste items were present in the 31 images. The deep learning model managed to identify 23 of the 33 items, obtaining 69.7% in accuracy. Figure 2.2 highlights the main limitation of the model, being unable to identify mixed waste items. Although the trained model was primarily focused on plastics, such findings suggest that the application of using deep learning models and image vision for real-life tossed waste materials remains limited.

2.7.2 Light reflectivity analysis

Experiment: Reflectivity analysis of materials is a highly adopted technique to classify different waste types (27). We next classify materials using light reflectivity measured

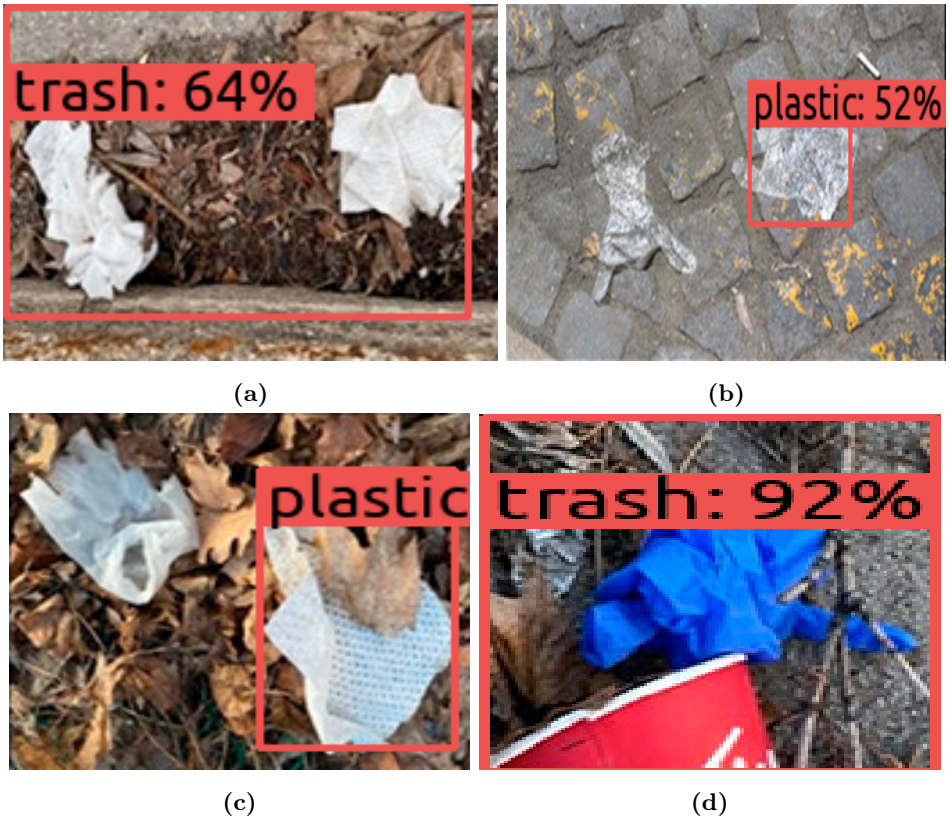

Figure 2.2: Trained model PlasticNet, discriminating plastics against other object materials (trash) (1)

through a photoresistor connected to the analog input pin of an Arduino MEGA ADK. The photoresistor captures light changes based on its resistance exposure to the light intensity of the reflected material. As a light source, we rely on a red laser diode (wavelength 650 nm). The object was located 2 cm away from the light source, depicting a practical usage of the sensor in transport belts and smart bins (13). We took measurements with the sensor for different materials (selection described in Section 3.2) during 1 min from two different places of the object selected randomly.

Results: Figure 2.3 depicts the results and compares them to two baseline backgrounds (white and black). We can observe that light can characterize different materials with low variations, but that different parts of the same material can be characterized very differently, e.g., Cardboard Cup-1 and Cardboard Cup-2. This is because end-products consist of different materials and colors, both affecting its properties. A key limitation

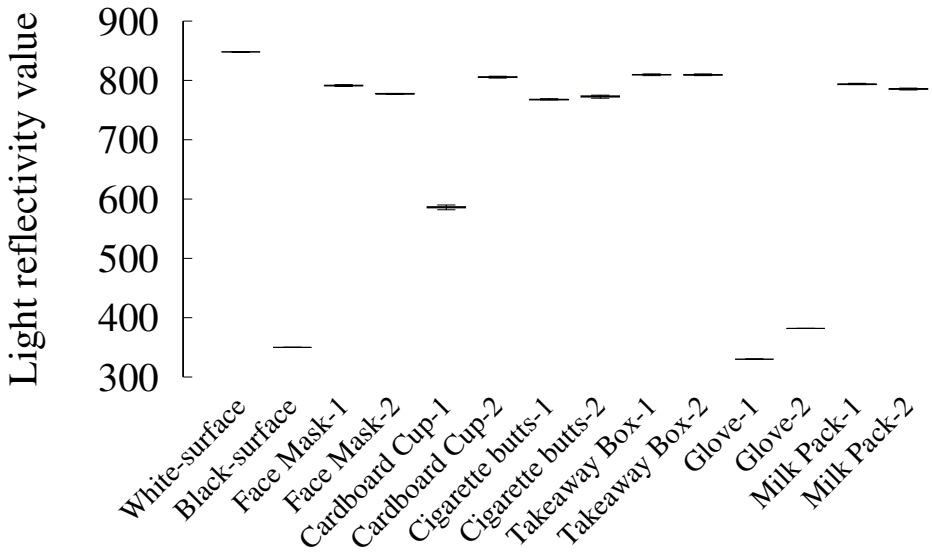

Figure 2.3: Light reflectivity values of different materials measured with a photo-resistor.

is that this approach requires a very short distance between the material and the sensor to classify the material accurately. Another limitation is that the light beam can cover a limited area, leaving most of the object untreated.

2.8 Summary

In this chapter, we presented a literature review about state-of-the-art passive sensing (IR thermal imaging). We introduced thermal cameras, which are used to perceive thermal infrared radiation that is invisible to the human eyes. There are different detection mechanisms for thermal cameras, with microbolometers and ferroelectric detectors primarily used to create thermal sensors that are uncooled. Although thermal cameras have their disadvantages, their strengths outweigh their limitations, one of which is their ability to see in dark or harsher conditions. Night vision systems, for example, act like the human eye; they identify and greatly magnify tiny quantities of visible light. Night vision cameras are wholly useless in a totally dark room, because the subject is completely blind due to no light source. Thermal cameras, on the other hand, do not

see visible light, but see heat radiation and sense material temperature variations that are reflected back by the object being measured.

Furthermore, we explored how state-of-the-art methods focused on computer vision and light reflectively fared as household waste was classified. Computer vision deep learning model managed to classify 23 of the 33 objects, achieving 69.7% accuracy. Reflective analysis of light shows that light could characterize various materials with low differences, but that it is possible to characterize other parts of the same material differently. The basic drawback of this method is that it requires a very small distance between the sensor and the material to reliably classify the material. Finally, by illustrating the significance and usefulness of this approach in a similar domain, we introduced the actual research in thermal sensing related to this study

To evaluate whether thermal radiation can be also used to classify different types of materials, in the next Chapter, we introduce multiple household objects and conduct an analysis to verify its feasibility.

3

Feasibility Analysis

This Chapter describes the most common classification of municipal solid waste (25). By selecting relevant waste items, we then conduct a controlled experiment to determine whether thermal imaging can be used to classify their material types. In particular, we analyze the fading time of residual thermal radiation that is acquired by the material object (waste) after being touched by a person.

3.1 Material selection

3.1.1 Plastic material

Plastic has become dominant in the consumer marketplace, which has been a useful and versatile material for various applications. Economic growth and increased demands on plastics have led to the accumulation of plastic solid waste (PSW) in landfills. They account for a large amount of municipal solid waste (MSW) in developed and developing countries, resulting in environmental problems. Packaging materials are designed for immediate disposal and constitute the largest market sector of plastic resins (71). With considerably different types of plastics, such as Polyethylene terephthalate (or PET), High-density polythene ($0.941 \leq$ density <0.965), Polyvinyl chloride (or PVC), Low-density polyethylene (LDPE) and Polypropylene (PP), Polystyrene (PS). PET belongs to the polyester family and is used in beverage, food, and other liquid containers. On the other hand, HPDE is a thermoplastic material composed of carbon and hydrogen atoms joined together forming high molecular weight products, can withstand higher temperatures, and are usually have a stronger intermolecular force and tensile strength

than LDPE (0.910 <density <0.925) (72). Cellulose acetate, a form of plastics are found in a cigarette with filters, which makes it almost impossible to decompose within a short period (73).

3.1.2 Rubber material

Rubber is of different types such as nitrile, silicone, natural rubber (NR), fluorocarbon rubber, styrene-butadiene rubber (SBR), ethylene-propylene-diene monomer (EPDM) rubber (74). There is an increase in rubber waste globally due to the never-ending demand for rubber products and usage in household products, medical, engineering, industrial, etc. Furthermore, rubber in so many applications has resulted in a growing volume of rubber waste, which poses major environmental problems, as the constant increase of discarded rubber makes disposing of rubber products worse. We all have a responsibility in making sure various forms of waste are discarded appropriately. For example, disposed rubber gloves in garbage has contributed to the amount of waste rubber generated worldwide (75), which could be attributed to a lack of environmental awareness in society. Sources of waste generated by rubbers include discarded rubber gloves, balloons, rubber bands, shoe soles, scrape tires, inner tubes, condoms, etc.

3.1.3 Glass and ceramic material

Based on its chemical composition, glass is classified into three types: soda-lime glass (which is widely used in making bottles and jars, Flat glass, Tableware), Pyrex or borosilicate glass is highly heat resistant (can resist thermal shocks for use in laboratories, Glass fiber, Wool insulation Ovenware), Lead crystal glass (used in Crystal tableware, Television screens, and display screen equipment) (76). However, glass containers and bottles are the most commonly used form of packaging beverages, food, and commodity items. This has contributed significantly to the municipal solid waste stream in our society. On the other hand, ceramic is used in making a variety of products ranging from tiles, cement, flower pots, etc. Just as glass, ceramic contributes to MSW in the environment and should be recycled adequately.

3.1.4 Metal material

Sophisticated metallic products with specific chemical and physical properties have been developed to satisfy basic human needs. Large quantities of metal waste emanate from the growing production and manufacture of goods and services for human comfort. Metal is among one of the pollutants, which cause severe threats to humans and the environment (77). Metals can be classified as ferrous, or non-ferrous. Metals that have an iron with carbon as its main constituent is considered ferrous. Ferrous materials are usually stronger and harder and are used in daily life products. Some common ferrous materials include alloy steel, wrought iron, carbon steel, cast iron, and Stainless steel.

On the other hand, non-ferrous metals do not contain a great amount of iron. Examples of non-ferrous materials are copper, aluminum, zinc, lead, Nickel, Tin etc (78). Globally, there has been a steady increase in demand for portable electronic equipment like mobile phones, cameras, Notebook, etc. This demand has led to an increase in lithium-ion batteries' production and consumption of lithium-ion batteries (79). Most phone batteries are made of metal elements such as lithium, cobalt, manganese (80).

3.2 Thermal emmisivity of materials

We next demonstrate that heat transfer of thermal radiation from humans can be used to opportunistically characterize different household objects. We demonstrate that the dissipation time of a thermal footprint correlates with the emissivity coefficient ϵ of different materials and can be used to characterize a wide variety of different objects. We measure the thermal footprint's dissipation using a thermal phone CAT s60, and a certified thermometer FLIR TG267. The measurement setup is described in detail in Chapter 5. Secondly, as different (mixed) materials form household objects, e.g., a cardboard cup is made with cardboard and coated with plastics or wax to prevent the absorption of liquids, we conduct experiments where the objects are held by a human hand for fixed periods before being placed on a plain surface so that the thermal footprint can be analyzed. We measure the thermal footprint dissipation time until the object reaches equilibrium with the ambient environment.

3.2.1 Thermal footprint dissipation

Testbed: We measure the dissipation time of a thermal footprint in different plastic materials, which correspond to standard resin identification codes (RIC). These plastics correspond to common materials, used in everyday plastic products and have well known emissivity coefficients (ϵ=0.90 - 0.97). We consider LDPE (Low Density Polyethylene), HDPE (High Density Polyethylene), PP (Polypropylene), PS (Polystyrene), and PVC (Polyvinyl chloride). The tested plastic samples are produced using the same mold cavity and identical manufacturing process[1]. Thus, samples' differences are directly proportional to their inherent material properties, e.g., material shrinkage and stiffness. In the experiments, we allocate the plastic sample inside a fridge with a constant temperature of 5℃, in order to achieve baseline temperature for comparison. Furthermore, we allocate a constant heat source (lamp bulb of 60 Watt) over the plastic sample - from a fixed distance of 10 cm to avoid burning the sample while exposing to enough thermal radiation. We heat the samples during different periods. Once a period is completed, we remove the heat source and measure the plastic sample's thermal footprint dissipation. Ambient temperature during experiments oscillated around 22-24℃.

Results: Figure 3.2 shows the results. From the figure, we can observe that a thermal footprint dissipates differently in different plastic materials. As periods to transfer thermal radiation from the lamp to the plastic sample, we selected 1, 2, 3, and 4 minutes. We did not consider further periods as 4 minutes was enough to show an association between dissipation time and the emissivity coefficient. Non-parametric Spearman correlation (81) indicates a significant positive relation between dissipation time and emissivity coefficient ($\rho = 0.66$, $p < .05$)

3.2.2 Thermal characterization with common household objects

Testbed: We measure the dissipation time of a thermal footprint from various household objects. We consider common household objects in our experiments that account for a large amount of solid municipal waste (68). The objects are shown in Figure 3.1 and cover a wide variety of highly discarded pollutants, including, rubber, plastics, glass, ceramic and metal. The considered objects include: a beer can (A), ceramic cup (B), takeaway box (C), plastic bottle (D), glass bottle (E), coffee cup (F), plastic cup

[1]https://www.materialsampleshop.com/products/plastics-sample-set

Figure 3.1: Selected waste materials for preliminary experiments. A (Beer can), B (Ceramic cup), C (Takeaway box), D (Plastic bottle), E (Glass bottle), F (Coffee cup), G (Plastic cup), H(Cigarette butt), I (Glass jar), J (Milk pack), K (Aerosol can), L (Rubber glove), M (Metal spoon), N (Face mask).

(G), cigarette butt (H), glass jar (I), milk pack (J), aluminum aerosol can (K), rubber glove (L), steel spoon (M) and a face mask (N). We analyze the thermal dissipation time after the objects held for $1, 2, 3$, and 4 min. The average body temperature of the human subject holding the object was around $35 - 36$℃. The ambient temperature was around $22 - 24$℃. We measure the dissipation of the thermal footprint using a thermal phone CATS60, and a certified thermometer CAT TG267. A detailed description of the apparatus is provided in Chapter 5.

Results: Figure 3.3 and 3.4 shows the results. Friedman test using dissipation times and object materials as experimental conditions showed significant differences for thermometer scanner ($\chi^2(2) = 48.54$, $p < .05$, $W = 0.93$) and CAT s60 ($\chi^2(2) = 48.83$, $p < .05$, $W = 0.93$). This suggests that thermal footprint's dissipation time is different for different materials.

3.3 Summary

This chapter presented a preliminary analysis of the thermal dissipation of materials. We measured the dissipation time of a thermal footprint in various plastic materials when placed in the fridge for a period. The plastic is placed 10cm away from a 60watts lamp to expose it to thermal radiation. The plastics examined were everyday plastics products for daily use, with a high level of emissivity coefficients. We considered LDPE

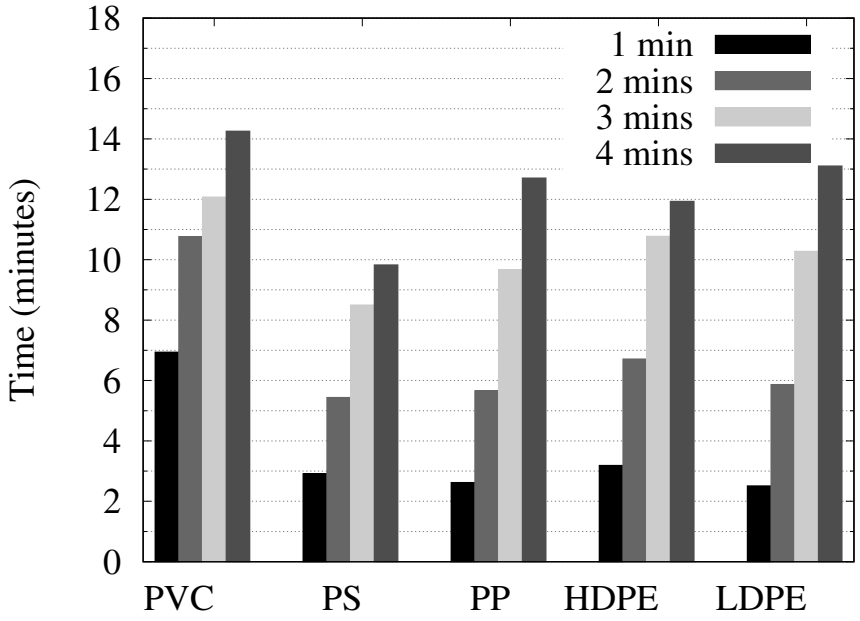

Figure 3.2: Dissipation time of thermal footprints in different plastic materials and used two different devices

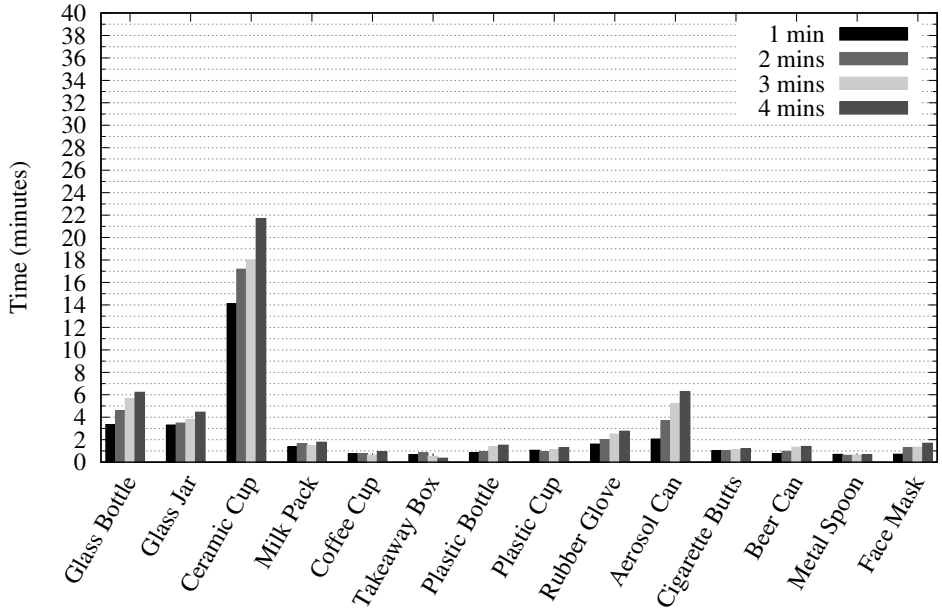

Figure 3.3: Dissipation time of thermal footprints in thermometer scanner TG267 (baseline)

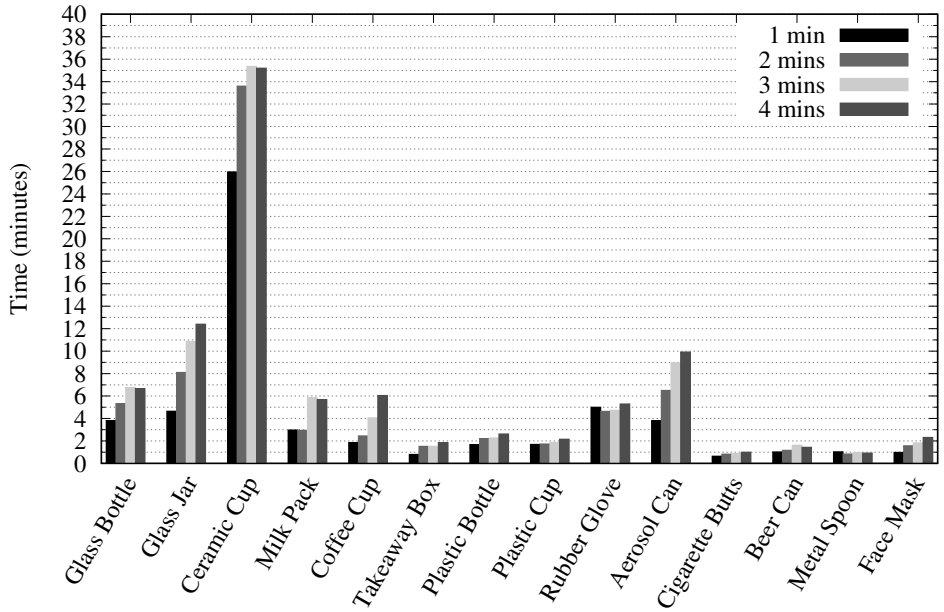

Figure 3.4: Dissipation time of thermal footprints in Smartphone CAT s60

(Low-Density Polyethylene), HDPE (High-Density Polyethylene), PP (Polypropylene), PS (Polystyrene), and PVC (Polyvinyl chloride). The result of the experiment shows that a thermal footprint dissipates differently in different plastic materials.

We also conducted a feasibility analysis using common household objects used in everyday life and account for large amounts of solid municipal waste. To determine the material thermal footprints' dissipation time, a controlled experiment was conducted. We analyzed the thermal dissipation time after the objects are held for 1, 2, 3, and 4 minutes. We measure thermal footprint dissipation via a thermal phone CAT S60 and a certified thermometer CAT TG267. Our findings show that various object materials may be distinguished by human-emitted thermal radiation. We also show that the dissipation time of a thermal footprint coincides with the coefficient of emissivity ϵ of different materials and can be used to identify a wide variety of other objects.

With this information, in the next Chapter, we then proceed to model the dissipation time of thermal footprint that are acquired from residuals of thermal radiation emitted by humans.

4

Modelling Thermal Footprint Dissipation

This chapter introduces the thermal image processing pipeline used to develop a model that classifies object materials based on thermal footprints' dissipation time.

4.1 Pre-processing of thermal video footage

Besides the lack of accuracy to measure temperature (82), thermal cameras in smartphones also suffer from several other issues. In particular, misalignment between thermal and RGB pictures and periodic re-calibration of thermal radiation introduce noise in continuous monitoring activities, e.g., black and white frames. To reduce the impact of noise in our thermal video footage, we transform videos into a sequence of thermal images. We then examine consecutive images based on background information to spot dissimilarities between images. Note that we remove the images with noise.

4.2 Normalization

Once the measurements were noise-free, the thermal pictures are normalized to a consistent scale, such that a sequence of thermal footprints can be easily analyzed. We normalize thermal pictures to values between 0 and 255, such that thermal images can be manipulated at gray scale. Figure 4.1 illustrates the result of the normalization process. In the figure, we observe the sequence of thermal pictures and the equivalence in normalized scale for two cases, a) a cardboard cup and b) a cigarette butt. By doing

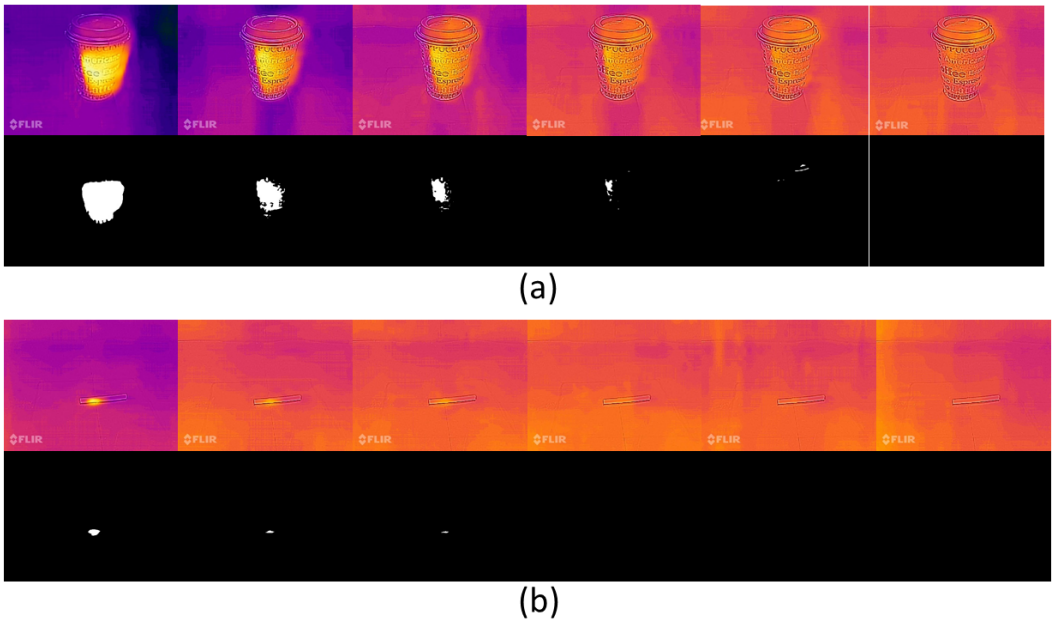

Figure 4.1: Dissipation time of thermal footprint for two different objects: a) Cardboard cup; and, b) Cigarette butt.

this, it is possible to isolate the thermal footprints of each object, as demonstrated in the figure.

4.3 Dissipation rate

From the normalized sequence of pictures, we then estimate the dissipation rate of the thermal footprint as the function of area reduction, as shown in Figure 4.2. We estimate the reduction in area (83) of the thermal footprint given by the following equation:

$$RA = (A_i - A_t)/A_i, \tag{4.1}$$

where RA is the reduction area percentage, A_i is the initial area, and A_t is the reduced target area. Information on the reduction area between consecutive images is used to create vectors that model the dissipation time of thermal footprints for each object.

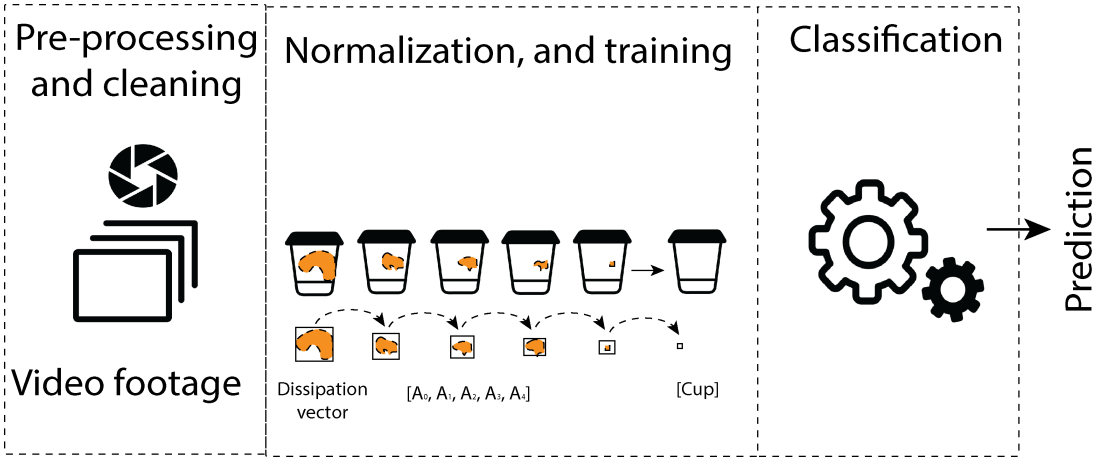

Figure 4.2: Processing pipeline of material classification based on dissipation time of thermal footprints.

4.4 Algorithm

In this thesis, we use machine learning classification algorithms based on Random Forest (RF) and Support Vector Machine, with deep learning technique Multi-Layer Perceptron to classify materials.

Random Forest (RF) also known as a Decision tree is a Tree-based classifier or predictor, where each classifier generated, depends on the values of a random vector sampled independently and with the same distribution for all trees in the forest (84). This supervised approach has proved to be an efficient tool, to name a few, in many fields such as medical imaging (85), bioinformatics (86), and identification of seeds in agricultural (87). RF utilizes Bagging also known as bootstrap aggregation which generates multiple versions of a predictor, for each node in the tree and chooses random features to merge prediction using majority vote when predicting class (as shown in Figure 4.3), or averaging when predicting regression (88).

On the other hand, **Support Vector Machine (SVMs)** is a predictive analysis data-classification algorithm for two groups' classification problems, it assumes the data in questions contains two possible values. Two-classes are linearly separable, the SVMs select the one linear decision boundary that leaves the greatest margin between the two classes (89). SVM algorithm has been used successfully in numerous applications, such

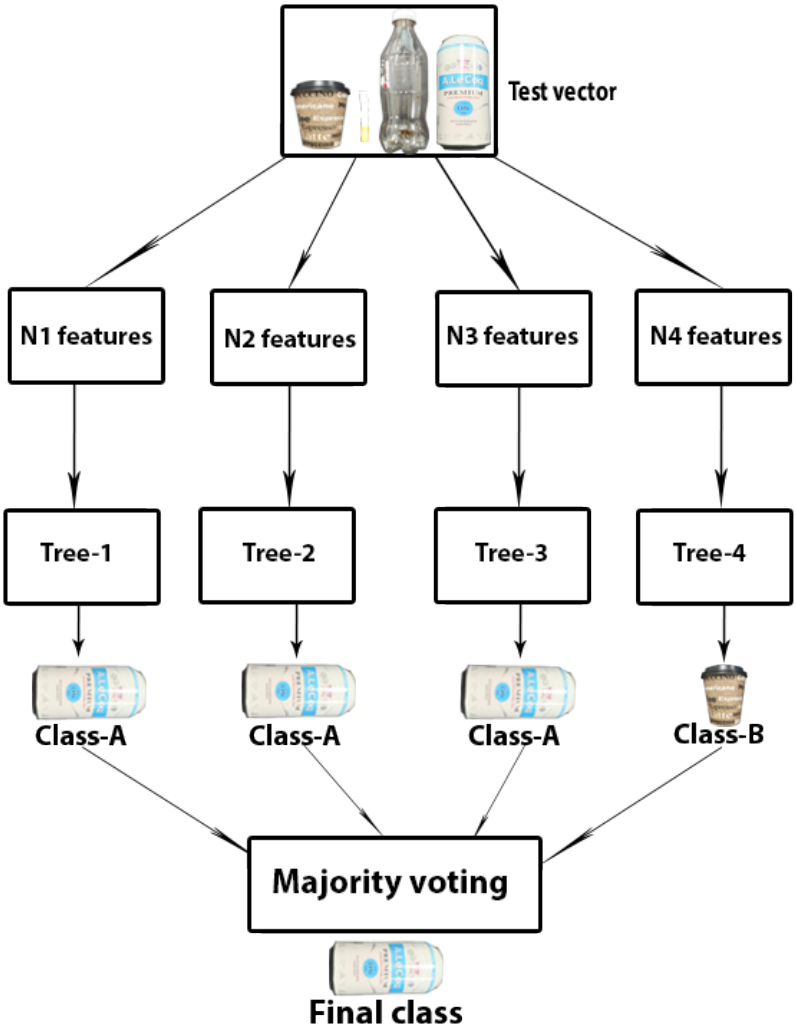

Figure 4.3: Structure of Random Forest Algorithm

as medical diagnosis (90), image recognition (91), and text analytics (92). For instance, in image recognition, if we design a predictive model that will predict the name of a fruit from a set of individual pictures without looking at it. Given an input vector, SVM classifies each picture and predicts what type of fruit appears.

In conclusion, the use of neural networks such as the **Multi-Layer Perceptron classifier (MLPC)** algorithm is an effective technique in contrast to more traditional statistical techniques (93). As in the case of random forest and support vector machine, MLPC can also be used for supervised learning of binary classifiers. The perceptron is considered a linear classifier because it makes its prediction by classifying input, by combining a set of weights with the feature vector. MLPC consists of at least three layers of nodes which are, an input layer, a hidden layer, and an output layer.

4.5 Implementation

We predict what type of object an individual interacts with based on its dissipation time. To achieve this, vectors with dissipation time are then used as classes that annotate the video footage. We develop classification models based on the algorithms mentioned above to classify objects based on their thermal footprints. All the vector have the same length and depict reduction of area from 1 to 0.

4.6 Summary

In this Chapter, by first pre-processing video recordings to eliminate the effect of noise; we turned videos into a series of thermal images. To manipulate images on a grayscale, pre-processed images are scaled to values between 0 and 255. The thermal footprint dissipation rate is then calculated from the normalized series of images as a function of area reduction. Also presented was an overview of the thermal image processing pipeline used to build a model that classifies object materials based on thermal footprints' dissipation time. The model is implemented using a machine learning algorithm random forest, support vector machine, and multi-layer perceptron classifier to classify materials.

To generalize our approach for different individuals, and materials, in the next chapter, we conduct a user study in a controlled testbed.

5

Thermal Dissipation Fingerprint Testbed

This Chapter discusses the protocol used in the user experiment and describes the experimental testbed designed to capture video footage of thermal footprints for different objects materials. For this purpose, we used an off-the-shelf smartphone thermal (CAT s60) camera and a thermometer scanner (TG267) to measure the reference baseline.

5.1 Participants

Since body temperature differs between individuals (94), to determine how a thermal footprint from various material dissipate when a user interacts with it for a while. We recruited a total of N=18 participants (Male=9, Female=9) for the user study. The participants were students, admin staff, and professionals from different fields and nationalities. Their average age was 28 years (standard deviation = 7.8). They had little or no knowledge about thermal imaging, as there was no such prerequisite.

5.2 Experiment design

We analyze the amount of thermal radiation transferred from a human hand to an object located in the surroundings. By quantifying the dissipation time of the thermal footprint, it is possible then to characterize different material properties of the object. The study follows a 3×3 within-subject design with thermal radiation transfer type and object type as independent variables. Both variables have three levels: {Fixed-hold

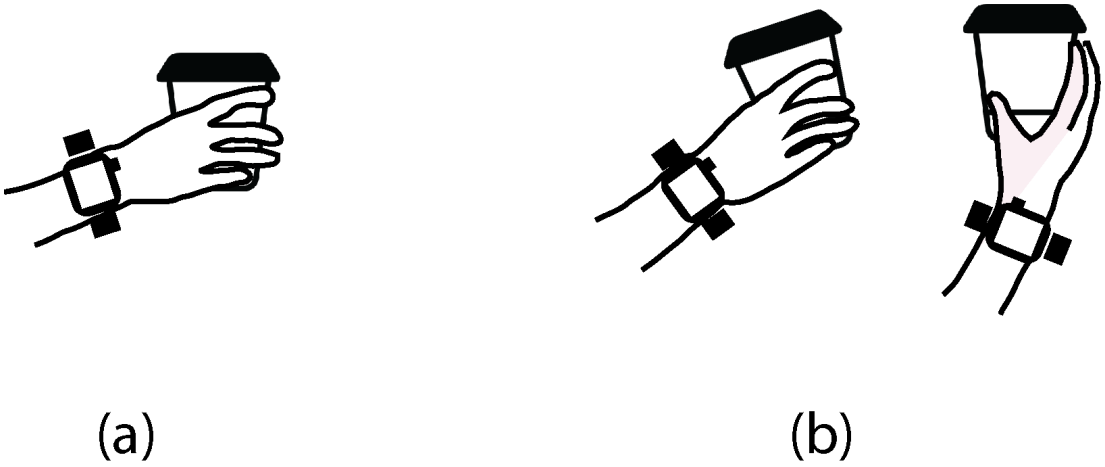

Figure 5.1: Exp. conditions. a) Rigid interaction (used in Fixed-hold), b) Free interaction (used in Natural and Quick holds)

(FH), Natural-hold (NH) and Quick-hold (QH)} for *thermal transfer type* and {Plastic bottle (BOTTLE), Cardboard cup (CUP) and Cigarette butt (CIGAR)} for *object type*. To eliminate order effects, but to keep the number of combinations manageable, thermal transfer type was fully counterbalanced whereas object type was counterbalanced following a Latin Square design, resulting in nine experimental conditions: BOTTLE-FH, CUP-FH, CIGAR-FX; BOTTLE-NH, CUP-NH, CIGAR-NH; BOTTLE-QH, CUP-QH, and CIGAR-QH.

Under the *Fixed-hold* condition, objects were held from a specific static position during 1 min (Figure 5.1a). For the *Natural-hold* condition, objects were held in a free manner during 1 min, simulating normal interaction with the objects (Figure 5.1b). For instance, a participant holds the empty bottle for one minute while looking for a trash bin. For the *Quick-hold* condition, objects were held by participants in a free manner during a brief span of 10 s.

Our final design includes 18 participants $\times$ three thermal transferred conditions $\times$ three object materials = 146 trials.

5.3 Apparatus

We rely on a handheld thermal imaging scanner (FLIR TG267) and a Caterpillar smartphone (s60) with integrated thermal imaging cameras. Both devices are capable of

measuring thermal temperature directly from the surface of materials. Handheld thermal imaging scanner main features included: IR resolution of 160×120 pixels, Focal plane array/spectral range-Uncooled microbolometer/$7.5 - 14\mu m$, Image frequency of 8.7Hz, Object temperature range -2°C to 380°C (-13°F to 716°F) and Thermal sensitivity(NETD) <70mk (milliKelvins). Similarly, the CAT s60 main features are thermal Resolution (Pixels) 60×80 pixels, temperature Range -20°C to 120°C, thermal sensitivity (MRDT) 150mk, accuracy typically ±5°C or ±5% of the difference between ambient and scene temperature, thermal sensor $17\mu m$ pixel size, $8 - 14\mu m$ spectral range. The CAT s60 camera was placed on a tripod at a distance of $30 - 35$ cm from the object and calibrated after thermal equilibrium has been attained when exposing to the room temperature of $22 - 23.5$℃. Video footage was recorded with the CAT s60, while thermal reference photos were taken with the TG267. Before starting the experiment, the participants' body temperature was collected using a clinical certified light thermometer (DRCHECK FC500). The room's ambient temperature was collected using a Netatmo weather station (`https://www.netatmo.com`). We also collect the dissipation time of the thermal footprint manually using a stopwatch timer.

5.4 Task

The participants were asked to hold object materials, simulating normal interactions with objects. They also contextualized themselves into normal situations while respecting the thermal transferred condition of the experiment. When interacting with the BOTTLE, participants were asked to simulate consuming the bottle's content and then looking for a trash bin to dispose of the empty waste. Similarly, the participants were asked to stand while engaging in a short conversation with an acquaintance/friend, for the CUP. Finally, for the CIGAR, the participants were asked to simulate taking a cigarette from a cigarette box, and then holding the cigarette from the filter while asking for light - cigarette was not lighted during the experiment.

5.5 Procedure

The procedure of thermal radiation transferred between a human hand and the household objects is illustrated in Figure 5.2. Before the experiment started, the participants

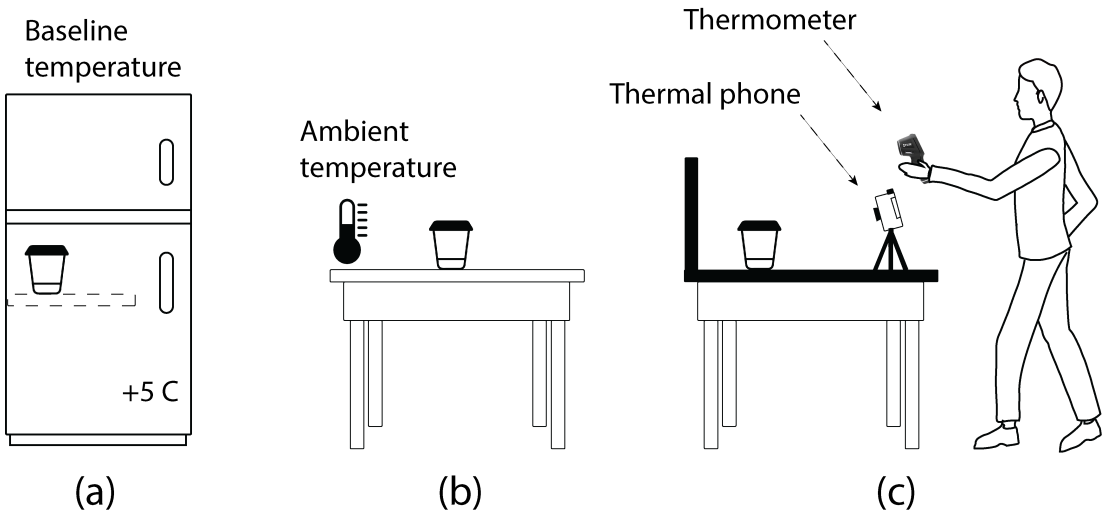

Figure 5.2: Experimental testbed and protocol steps. a) Object obtains baseline temperature, b) Object habituates to ambient temperature, c) Participant performs the experiment and puts the object in the marked target to measure its thermal footprint.

were asked to relax on a comfortable chair for 10 minutes to enable the body temperature to acclimatize to the room's ambient temperature, which oscillated around $22 - 23.5$℃ throughout all the experiments. During this period, the participants also received an explanation of the purpose of the study. They also signed an informed consent form, following the regulations of our University. The participants were presented with a sequence of nine experiment conditions discussed previously. This sequence was counterbalanced to avoid any possible order effect. At a time, one participant performed the whole experiment. The evaluation took place in one university room across two weeks in time slots that fall within the interval of 11:00 am to 07:00 pm. Since human temperature varies during the day (94), we consider these times only as these times depict working hours for the participants. For each participant, the overall experiment lasted around $45 - 50$ minutes.

Before the study begins, the participant's body temperature is taken from the forehead using the clinical light thermometer. After that, the participant started the experiment, and one condition was presented at the time until completing the nine experiments. Each object was located inside an empty fridge with a temperature of 5℃ during 1 min (as shown in Figure 5.2a). This procedure rules out residual thermal radiation in the material between experiments and provides the material with a baseline temper-

Figure 5.3: Experimental testbed.

ature to make our results comparable among participants. The researcher conducting the experiment used kitchen tongs to put in and take the object from the fridge to avoid transferring his/her human thermal radiation. Next, the object was then placed on a table for 1 min, so that it adapts to the ambient temperature (as shown in Figure 5.2b). After this, the participant took the object from the table and performed one of the experiment conditions following a task described previously. Next, the participant put the object on a fixed marker drawn on a table with a black background and surface (as shown in Figure 5.2c and Figure 5.3). The researcher used the CAT s60 to record video footage of the dissipation of the object's thermal footprint. Simultaneously, a thermometer scanner took thermal photos during this time to serve as the reference baseline. The black background helps to obtain clean video footage from the thermal footprint without any thermal influence from any other object in the surrounding environment. At the end of the experiment, the participant's temperature from hand palm and finger was measured using the thermal imaging scanner (as shown in Figure 5.4). Devices were allowed to cool down for a couple of minutes after each experiment to avoid heating up.

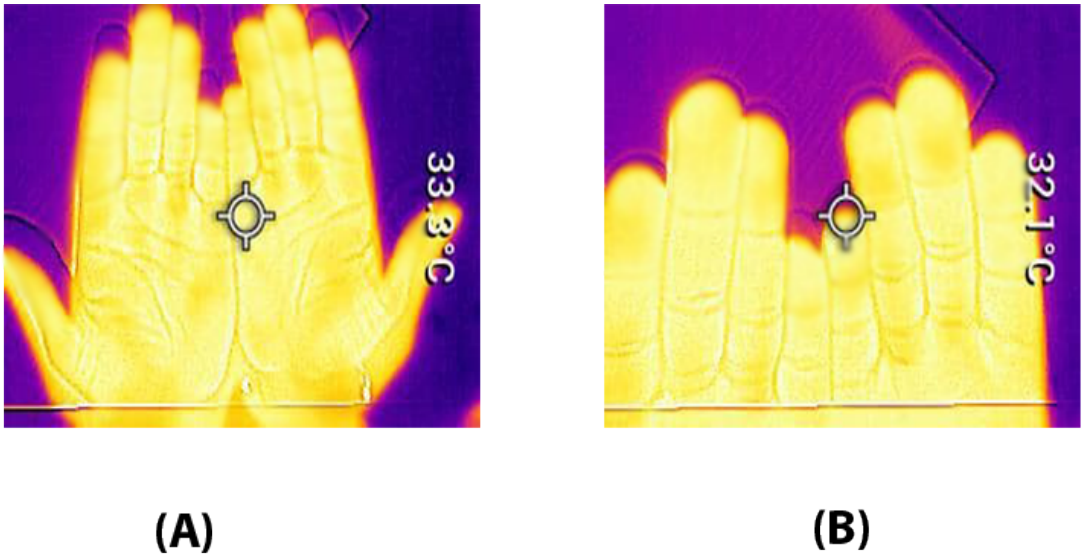

Figure 5.4: Thermal radiation of a participant (a) hand-palm (b) finger-tips. To preserve the identity of the individual, the images were distorted.

5.6 Summary

In this Chapter, we performed a user study with several participants to generalize our proposed approach. We used three different materials for the research for two reasons. The first is to have objects evaluate different other variables, such as form and scale. The second explanation is that materials whose dissipation time is not too long are selected so that the experiment is not boring for participants and decreases the chance of noisy results.

In the next chapter, we present our findings.

6

Analysis and Results

We evaluate MIDAS on different object materials. We conduct a controlled study with multiple participants in a lifespan of two weeks. The objective is to determine whether it is possible to use human-emitted thermal radiation to characterize different objects. By relying on different human subjects, we expect to learn whether our approach can be generalized across different objects and users. We use Wilcoxon, the Friedman, and Dunn-Bonferroni statistical test to detect treatments across multiple test attempts. These statistical tests are non-parametric, which can be used to test or compare the difference between paired groups.

6.1 Differences in human temperature

Figure 6.1 shows the body temperatures from all the participants for different body parts. The average body temperature for each of them was, forehead 36.33℃, hand-palm 30.16℃ and finger-tips 30.87℃. Friedman test using body parts as experimental conditions showed significant differences for temperature ($\chi^2(2) = 29.66$, $p < .05$, $W = 0.82$). Posthoc comparisons (Dunn-Bonferroni) verified that the differences for body parts were statistically significant (p-value $< .01$) between forehead/hand-palm and forehead/finger-tips. From the results, we can observe a difference of $4-6$℃ between forehead and hand-palm/finger-tips, and higher variance for hand-palm/finger-tips measurements. This can indicate that hand-palm/finger-tips are more sensitive to ambient temperature changes and can also capture more indirect insights about the activities users perform. For instance, the battery temperature from a smartphone can induce a

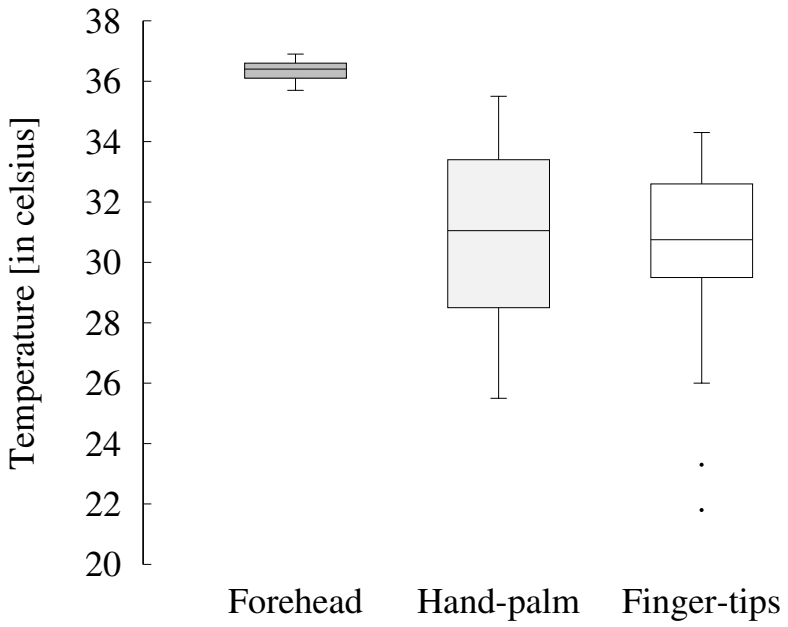

Figure 6.1: Body temperature of the participants.

higher temperature in an individual, indicating the level of smartphone usage (95). Induced temperature can help situations where the environment inhibits human-emitted radiation transferred to object materials, e.g., temperatures below 0℃.

6.2 Human-emitted thermal radiation to object materials

We analyze thermal radiation transferred from hand-palm/finger-tips to object materials as thermal footprints by measuring the dissipation time of the thermal footprint under three experiment conditions (Fixed-Hold, Natural-Hold, and Quick-Hold). Figure 6.2 shows the dissipation time for all the conditions. Friedman Test using dissipation time and objects as experimental conditions shows significant differences fixed-hold ($\chi^2(2) = 20.33$, $p < .05$, $W = 0.56$), natural-hold ($\chi^2(2) = 30.33$, $p < .05$, $W = 0.84$) and quick-hold ($\chi^2(2) = 25.04$, $p < .05$, $W = 0.64$). Pairwise Wilcoxon test verifies that dissipation time between different objects also were statistically significant in all the conditions. Our results indicate that enough thermal radiation can be found in hand-palm/finger-tips to characterize different materials for all conditions. These results also suggest that object materials can be fingerprinted without relying on any

specialized technology, but instead, just by relying on a simple human touch with much anticipation. The potential of this is that objects that are fingerprinted do not need to pass through complex waste management routines to obtain its material characteristics.

6.3 Differences between thermal transferred conditions

We have demonstrated that it possible to characterize objects with thermal human-emitted radiation under diverse experimental conditions. This section analyzes the differences in the characterization of the same object between different conditions to determine the factors that influence the characterization process. Friedman test using dissipation time of each object and the three experimental conditions shows significant differences only for the plastic bottle ($\chi^2(2) = 12.44$, $p < .05$, W=0.34) and the cupboard cup ($\chi^2(2) = 16.48$, $p < .05$, W=0.45). Wilcoxon test confirms significant differences between thermal transferred conditions for plastic bottle (fixed/quick and natural/quick) and cupboard cup (fixed/quick and natural/quick). The results suggest that the characterization of the object with thermal radiation is not tied to an unnatural manner of interacting with objects nor a specific area location in the object (e.g., since the cigarette-butt's overall size is small, the thermal radiation is concentrated and retained in a specific area). The absorption of thermal radiation for some objects (e.g., plastic bottle) is slow and depends on the exposure time. Conversely, this result indicates that the location is not a relevant factor (as long as the material is the same) to quantify the dissipation time. Thus, thermal radiation can be used to characterize objects that are held naturally by people. In general, our results indicate that characterization of objects with thermal radiation depends on the exposure time and does not depend on the location or area that the thermal radiation can cover and that natural interactions with objects can be exploited to identify materials with thermal radiation.

6.4 Other factors that influence thermal dissipation

We thus far showed that the characterization of object materials with thermal radiation highly depends on time. This section analyzes other factors that influence the transfer of thermal radiation from the human body to objects.

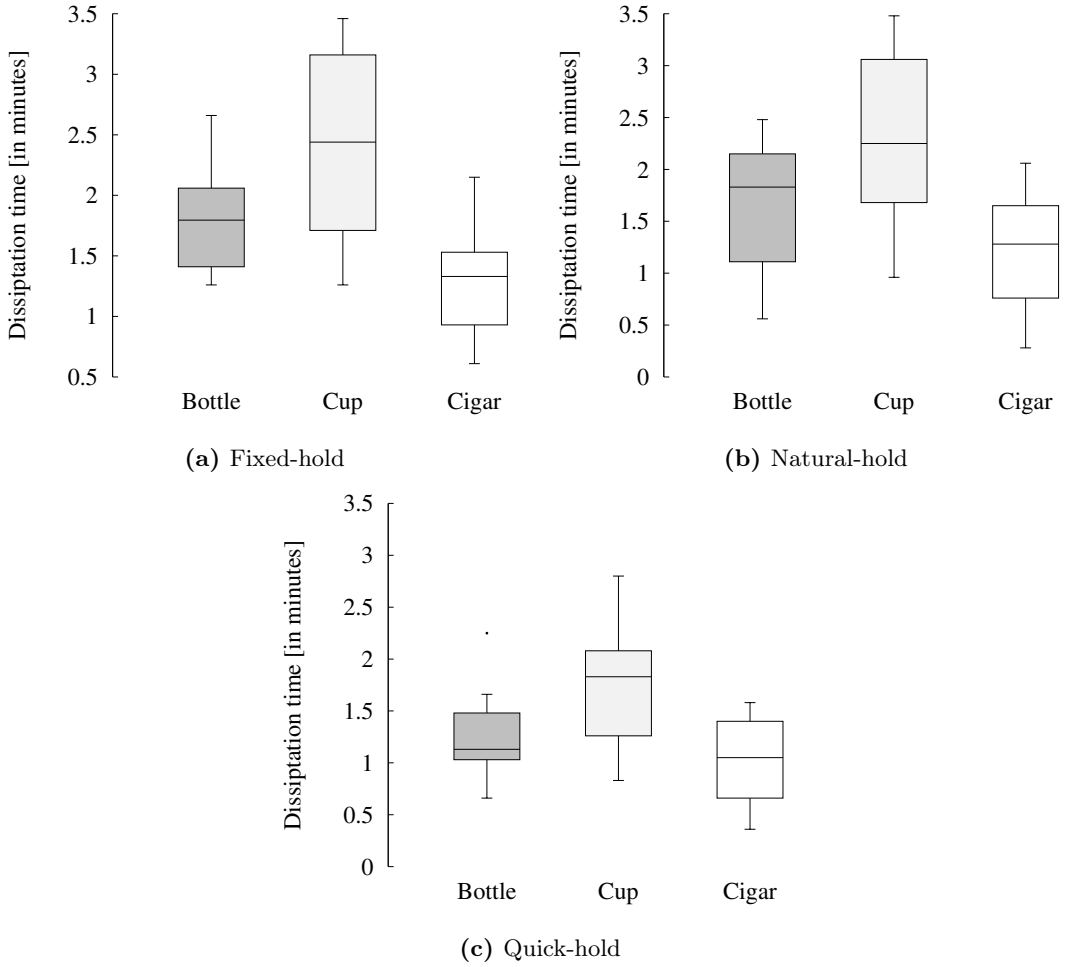

(a) Fixed-hold

(b) Natural-hold

(c) Quick-hold

Figure 6.2: Thermal transferred conditions applied over three different objects (Plastic bottle, cardboard cup, cigarette but)

Female vs male temperature: As body temperature directly influences the thermal radiation transferred to objects, we analyze whether temperature differences between female and male participants were significant for thermal transfer. Figure 6.3 shows the results for each body part, forehead, hand-palm, and finger-tips. Kruskal-Wallis test using gender and body parts as experimental conditions shown that there are significant differences only for finger-tips ($\chi^2(2) = 5.08$, $p < .05$). When using gender and objects as experimental conditions, Kruskal-Wallis shows there are significant differences in the dissipation time for cigarette-butt ($\chi^2(2) = 3.94$, $p < .05$), plastic bottle ($\chi^2(2) = 12.17$, $p < .05$) and cardboard cup ($\chi^2(2) = 7.75$, $p < .05$).

These results indicate that the dissipation time of the thermal footprint depends on temperature and that it is possible to identify whether a female or male individual has touched the object. While this result does not change the fact that objects can be characterized by thermal radiation, it is important to highlight that thermal radiation can disclose additional information about the people disposing of waste. For instance, it could be possible to identify persuasive stimuli that make females or males more prone to dispose of waste in the right recycling trash bin.

External temperature of ambient environment: The surrounding temperature of the object directly influences the dissipation time of the thermal footprint. To quantity the influence of this factor, we conduct further experiments, where the BOTTLE was held by a human hand for different periods in an ambient temperature $22 - 23.5$℃ and next, the BOTTLE was placed inside a colder environment (fridge with a constant temperature of 5℃ degrees). We then measure the dissipation time of the thermal footprint when changing from ambient to a colder environment using CAT s60 and the thermometer scanner. Figure 6.4 shows the results. We also include the thermal footprint's dissipation time in the ambient environment for comparison purposes (baseline). We notice that the dissipation time of the thermal footprint reduces by half when changing from ambient to a colder environment. This suggests that the environment is a key factor to monitor when relying on thermal footprints to fingerprint materials.

Internal temperature absorbed from other objects: Besides the ambient temperature of the surrounding environment, objects can also be influenced by the thermal radiation of the inside materials. For instance, a cardboard cup is with hot and cold coffee. To verify this, we conduct further analysis in which the BOTTLE object is filled fully with water with a temperature of $21.2 - 21.5$℃. Before the experiment, we located the filled water BOTTLE inside a fridge (5℃ degrees) to eliminate thermal radiation between experiments. We then compare the dissipation times of the empty and filled bottle's thermal footprints in ambient temperature ($22 - 23.5$℃ degrees). Figure 6.4 shows the results. We observe that the influence of internal radiation drastically disrupts the thermal footprint of the BOTTLE material. This is relevant to identify end-products that are discarded without consuming its goods. Thus, it should be treated with different separation protocol to avoid the contamination of pure materials. When compared with the thermal footprint of the empty BOTTLE, we can observe that the thermal footprint of the filled water BOTTLE dissipates faster. This is because the

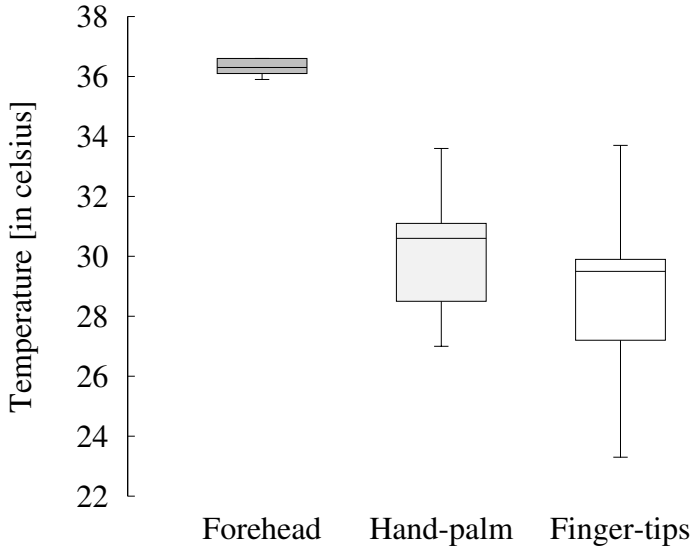

(a) Female participants

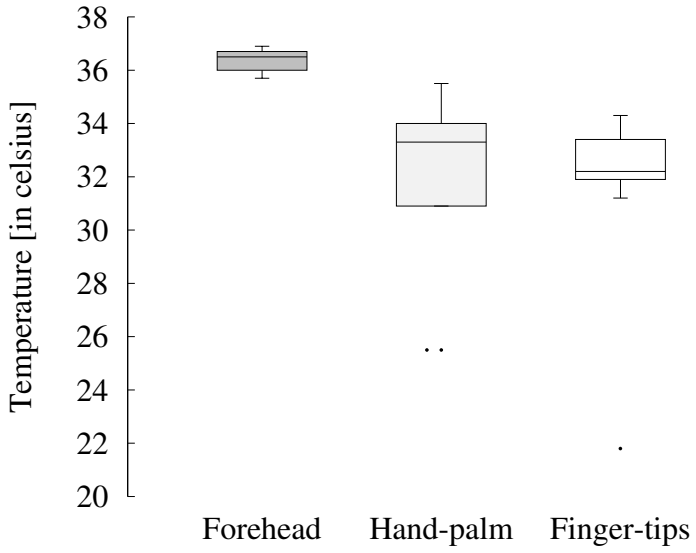

(b) Male participants

Figure 6.3: Differences in body temperature parts for female and male participants.

water became colder with time from the acquisition of the baseline temperature, and colder water accelerated the BOTTLE's dissipation time.

Distance between object and thermal camera: So far, the distance between the thermal camera and the object material has been around $30 - 35$ cm (baseline) in all

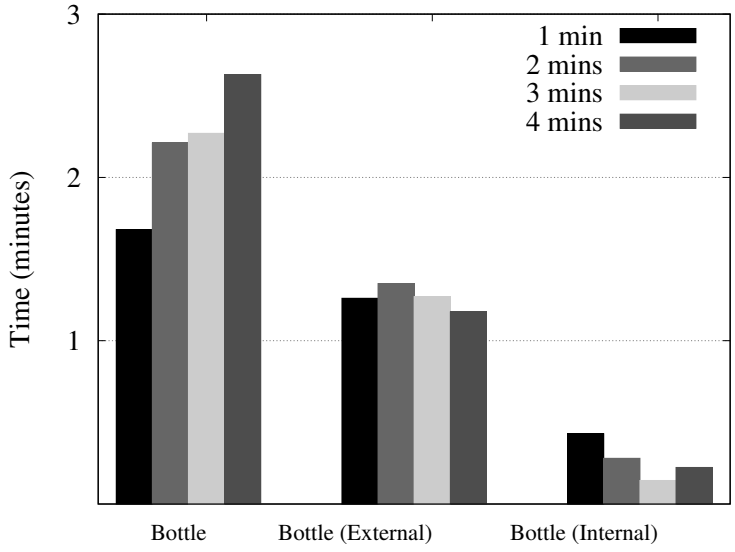

(a) CAT s60

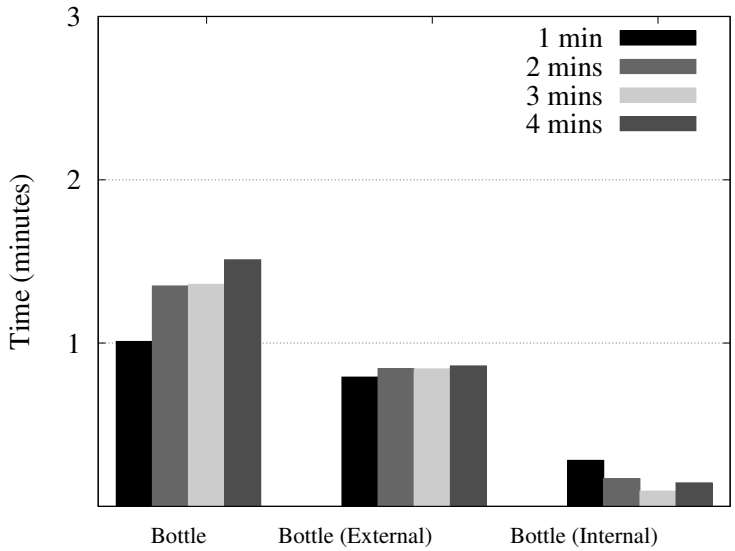

(b) Thermometer Scanner

Figure 6.4: Influence of internal and external temperatures.

experiments. We analyze with three different distances, distance-1 (70 cm), distance-2 (105 cm,) and distance-3 (210 cm), to quantify the influence of distance. We chose these distances as they enable us to measure thermal footprints from both CAT s60 and thermometer scanner. We rely on the BOTTLE material with a fixed-hold of 1 min

condition. By using the CAT s60, we found that at distance-1, the dissipation time does not change significantly (average time = 1.13 min). With higher distances, we observed higher variations in the dissipation time with CAT s60, distance-2 (average time = 0.76 min) and distance-3 (average time = 0.26 min). However, we could not observe even a thermal footprint from distance-3 using the thermometer scanner. This indicates that with the off-the-self thermal cameras, the maximum range to use our approach is about 1 m, which is enough for equipping trash bins and transport recycling belts with our approach. This maximum range also is higher than the existing light reflectivity-based techniques. Notice that this limitation can be overcome by using high-resolution thermal cameras. However, this in turn increases the practical cost when using the approach.

6.5 Dissipation time classification performance

Lastly, we demonstrate that our approach can support the coarse-grained classification of object materials based on the dissipation time of thermal footprints and other contextual factors. The results of the classification experiments are shown in Table 6.1. The estimation accuracy is around 83% when only the dissipation time of the thermal footprint is available to predict the material type. We can observe that hold type (Natural, Fixed) are not informative parameters as the accuracy remains the same. In contrast, when having information about the person is male or female, we can observe that the accuracy to predict materials improves up to 86%. More detailed results of the experiment are in the Appendix 9.

Likewise, when predicting the contextual hold type and whether the user is male/female, we can observe that dissipation time and material information provide a high accuracy estimation of around 78%. This is relevant for fostering the learning of autonomous systems based on interactions and personal characteristics of users. For instance, intelligent toys can change color based on female and male preferences.

6.6 Other use cases: Detection of abnormal human temperature

The previous sections demonstrated that human-emitted thermal radiation helps to characterize an object's material from its surface and that the amount of thermal radia-

Table 6.1: Material classification accuracy (%) in different experimental conditions. Model data → Predicted. Classification Method: Random Forest (RF), Support Vector Machine (SVM), Multi-layer Perceptron (MLPC).

Test	RF	SVM	MLPC	Average
Predicting Material (M)				
(Vector) →M	90.9	77.3	81.8	**83.3**
(Vector, Context)→M	90.9	77.3	81.8	**83.3**
(Vector, Gender)→M	90.9	86.4	81.8	**86.4**
(Vector, Context, Gender)→M	86.4	81.8	81.8	**83.3**
Average	*89.8*	*80.7*	*81.8*	***84.1***
Predicting Context, Gender				
(Material, Vector)→Context	77.3	81.8	72.7	**77.3**
(Material, Vector)→Gender	77.3	77.3	81.8	**78.8**
Average	*77.3*	*79.6*	*77.3*	***78.1***

tion absorbed by the object varies from individual to individual. We next demonstrate that our approach is not limited to supporting and optimizing waste management solutions but can enable novel and innovative sensing applications. As an example of such applications, we demonstrate how dissipation time variations can be used to detect variations in human temperature. Direct monitoring of human temperature using thermal cameras is only feasible on expensive high-resolution cameras that are taken from a specific region of the face (96). Our approach overcomes these requirements by using indirect measurements obtained from thermal dissipation fingerprints.

6.6.1 Experimental setup

We analyze further the BOTTLE material that we used in our previous experiments. To induce a controlled temperature in the object, we rely on an incubator JANOEL18S with adjustable temperature. We put the object inside the incubator at a constant temperature of 15 min to ensure that the entire object depicted the same temperature. We exposed the material to temperatures ranging from 36℃ to 39℃ degrees. We chose these temperatures as they depict normal and elevated temperature levels in a person. After the object was heated up, it was transferred to the testbed as depicted in Fig-

ure 5.2c and described in Chapter 5. We then proceed to measure the dissipation time of the thermal footprint. The room temperature that the object had to acclimatize ranges from 23℃ to 23.5℃ degrees. We recorded video footage of the dissipation time using a CAT s60 smartphone.

6.6.2 Results

We obtained the next results of dissipation time for different temperature degrees (3.33 min for 36℃ , 3.73 min for 37℃ , 4.23 min for 38℃ , and 4.34 min for 39℃ respectively). After the object was taken out from the incubator, its temperature dropped drastically from 36℃ degrees to $33-32$℃ in a fraction of a second. Nevertheless, the thermal footprints take different periods to dissipate when exposed to different temperatures. In the figure, we can observe that dissipation time is shorter when the temperature difference is smaller. The dissipation time increases as the temperature difference increases (it takes 1.2 min longer for the temperature to fade when comparing 36℃ against 39℃ degrees). Our results indicate that small differences can be detected through thermal footprint analysis. While accurate human temperature is not possible to estimate, we envision that our approach can be used to detect abnormalities in human temperatures. For instance, in an airport, instead of monitoring the face of people with thermal cameras, it can be possible to monitor the tangible objects that people touch while passing a security check. These could provide more insights on whether the person presents abnormal levels of temperature.

6.7 Summary

We developed a predictive model to characterize different objects based on its dissipation time using human emitted thermal radiation under different experimental conditions. We measure their statistical variations using Wilcoxon, the Friedman, and Dunn-Bonferroni test to assess if thermal radiation's dissipation period for different object materials is different. Our findings show that the dissipation time for multiple objects is statistically different after being subjected to a fixed-hold environment. We also compared differences between thermal transferred conditions, the findings show that the characterization of the object with thermal radiation is not related to an unnatural way of interacting with objects or a particular region. Our approach was also

able to identify the subject's gender whether a female or male individual has touched the material, the result shows that the thermal footprint's dissipation time depends on temperature. The ambient environment's external temperature also influences the dissipation time, as the environment is a crucial factor in monitoring fingerprint materials as they depend on thermal footprints.

In the next chapter, we discuss the implications and limitations of our work.

7

Discussion

This Chapter discusses the implications and limitations of our work.

7.1 Human temperature

Human temperature behaves in cycles, being at its highest peak during the day (hours of activity) and lowest peak during the night (sleeping hours) (94). We demonstrate that such temperature measured during day hours can be used to characterize object materials.

7.2 Room for improvement

Accuracy and noise-free thermal images are a relevant problem to adapt our approach for continuous monitoring. There are types of materials whose thermal refraction is not visible as they reflect too much light. Thus, the thermal footprint is difficult to evaluate. These materials are usually used to preserve users' privacy, e.g., ATM keywords. We are also interested in analyzing the influence of material color in our approach. Besides, in our case about abnormal human temperature, we are interested in validating our findings with actual patients. However, we need access to clinical experts and additional permissions from our University ethics department to do this.

7.3 Micro-expressions through hand-touch

Micro-expressions are facial expressions captured in a fraction of time by cameras. Our work demonstrates that the thermal footprint of a hand-touch on an object has a life span that depends on how long the object was held. Thus, thermal analysis of human touch can be another approach for detecting micro-expressions, e.g., disgust and excitement. Similarly, micro-expressions through human-touch can be envisioned as an approach to measuring individuals' productivity at work.

7.4 Robots and autonomous devices

Thermal radiation analysis of touched objects by humans can be used to train different robots and autonomous devices about objects' material properties. By doing so, these devices can adjust their operations to interact better autonomously with objects from the surrounding environment. For instance, a robotic arm can rely on a camera to detect an empty bottle on a table. However, the arm's pressure to lift and put the bottle should be proportional to the bottle material. Otherwise, the robotic arm can break apart the bottle, e.g., plastic vs. glass bottle. Besides, since it is possible to differentiate thermal radiation emitted by female and male users, autonomous devices can adjust their interactions accordingly.

Furthermore, public littering is known as a problem around the world which questions the integrity of our environment (7). Identifying waste thrown away on the streets and public places due to ignorance or lack of littering facilities is a path in the right direction. There is no doubt that people have heard a lot about environmental problems, and they now want to hear a lot more about environmental solutions. One way to solve this problem is by integrating thermal sensors into autonomous drones and robots to aid in recycling of public waste on the streets. With human-emitted thermal radiation transferred when interacting with objects, these robots can identify materials as soon as they are disposed of in the wrong place or places they do not belong and discard them properly.

7.5 Augmented reality systems

Augmented reality systems that mix the real and virtual worlds can benefit from thermal radiation monitoring. By piggybacking the human-touch on objects, it is possible to recognize the materials of objects further. These objects are mapped to the virtual world by considering their inherent natural material properties, such as wood, concrete, glass, and plastic.

7.6 Other pervasive systems

Several other pervasive systems can benefit from our thermal approach. Health monitoring systems can track temperature from individuals while preserving their privacy by monitoring objects' thermal footprints instead of direct human measurements are taken from different body parts, e.g., forehead and hands. Similarly, new sensing modalities that pre-warm the materials to understand the composition in different environments can be envisioned, e.g., cold and underwater environments.

8

Summary and Conclusion

We developed MIDAS as an innovative sensing-based approach that uses human-emitted thermal radiation to classify different material waste types. MIDAS builds on the intuition that people need to touch objects when they are throwing them away, and these interactions result in thermal footprints on the object's surface. It is possible to fingerprint the materials right before their actual disposal by analyzing thermal footprints' dissipation time. We validated our approach through controlled experiments and conducted a user study with multiple participants to demonstrate that MIDAS can accurately and robustly categorize different household waste items. We created vectors with the dissipation time to classify materials and construct Random forest, support vector machine, and Multi-layer perceptron classifier models. When using this approach, materials' emissivity should be considered, as objects with low emissivity will mirror or reflect radiation from a nearby source.

We also compared MIDAS with state-of-art approaches based on computer vision and light reflectivity, demonstrating that MIDAS is more robust as it focuses on material characteristics rather than on shapes or other characteristics of the objects being detected. The maximum range of MIDAS is around one meter, which is more than enough for most practical use cases. We also demonstrated that the sensing principle used in MIDAS is not limited to applications in waste management, but the general idea of thermal dissipation fingerprint can support other innovative applications, such as detecting abnormal temperatures to support health applications.

8. SUMMARY AND CONCLUSION

About this work: This work is published in IEEE PerCom 2021 (97).

H. Emenike, F. Dar, M. Liyanage, R. Sharma, A. Zuniga, M. Hoque, M. Radeta, P. Nurmi, H. Flores: MIDAS: Sensing Residual Dissipation of Human-emitted Thermal Radiation, In Proceedings of the IEEE International Conference on Pervasive Computing and Communications (PerCom 2021), Kassel, Germany, 2021

Bibliography

[1] J. C. Prata, A. L. Silva, T. R. Walker, A. C. Duarte, T. Rocha-Santos, Covid-19 pandemic repercussions on the use and management of plastics, Environmental Science & Technology 54 (13) (2020) 7760–7765. ix, 14, 15

[2] R. Vadivambal, D. S. Jayas, Applications of thermal imaging in agriculture and food industry—a review, Food and Bioprocess Technology 4 (2) (2011) 186–199. xi, 9

[3] S. Kaza, L. Yao, P. Bhada-Tata, F. Van Woerden, What a waste 2.0: a global snapshot of solid waste management to 2050, The World Bank, 2018. 3

[4] P. Goel, Water pollution: causes, effects and control, New Age International, 2006. 3

[5] J. T. Powell, T. G. Townsend, J. B. Zimmerman, Estimates of solid waste disposal rates and reduction targets for landfill gas emissions, Nature Climate Change 6 (2) (2016) 162–165. 3

[6] L. A. Guerrero, G. Maas, W. Hogland, Solid waste management challenges for cities in developing countries, Waste management 33 (1) (2013) 220–232. 3

[7] S. N. Robinson, Littering behavior in public places, Environment and Behavior 8 (3) (1976) 363–384. 3, 52

[8] R. P. Schwarzenbach, T. Egli, T. B. Hofstetter, U. Von Gunten, B. Wehrli, Global water pollution and human health, Annual review of environment and resources 35 (2010) 109–136. 3

[9] R. Geyer, J. R. Jambeck, K. L. Law, Production, use, and fate of all plastics ever made, Science advances 3 (7) (2017) e1700782. 3

[10] T. Anagnostopoulos, A. Zaslavsky, K. Kolomvatsos, A. Medvedev, P. Amirian, J. Morley, S. Hadjieftymiades, Challenges and opportunities of waste management in iot-enabled smart cities: A survey, IEEE Transactions on Sustainable Computing 2 (3) (2017) 275–289. 4

[11] I. Ručevska, J. Seager, T. H. Schoolmeester, H. L. Gjerdi, L. Westerveld, et al., Gender and waste nexus: Experiences from bhutan, mongolia and nepal. 4

[12] A. A. Babaei, N. Alavi, G. Goudarzi, P. Teymouri, K. Ahmadi, M. Rafiee, Household recycling knowledge, attitudes and practices towards solid waste management, Resources, Conservation and Recycling 102 (2015) 94–100. 4

[13] G. White, C. Cabrera, A. Palade, F. Li, S. Clarke, Wastenet: Waste classification at the edge for smart bins, arXiv preprint arXiv:2006.05873. 4, 7, 13, 14, 15

[14] B. Esmaeilian, B. Wang, K. Lewis, F. Duarte, C. Ratti, S. Behdad, The future of waste management in smart and sustainable cities: A review and concept paper, Waste management 81 (2018) 177–195. 4

[15] X. Bing, J. M. Bloemhof, T. R. P. Ramos, A. P. Barbosa-Povoa, C. Y. Wong, J. G. van der Vorst, Research challenges in municipal solid waste logistics management, Waste management 48 (2016) 584–592. 4

[16] O. O. Fadare, E. D. Okoffo, Covid-19 face masks: a potential source of microplastic fibers in the environment, The Science of the total environment 737 (2020) 140279. 4

[17] J. M. Lloyd, Thermal imaging systems, Springer Science & Business Media, 2013. 4, 8

[18] M. Vollmer, K.-P. Möllmann, Infrared thermal imaging: fundamentals, research and applications, John Wiley & Sons, 2017. 4

BIBLIOGRAPHY

[19] H. Flores, J. Hamberg, X. Li, T. Malmivirta, A. Zuniga, E. Lagerspetz, P. Nurmi, Evaluating energy-efficiency using thermal imaging, in: Proceedings of the 20th International Workshop on Mobile Computing Systems and Applications, ACM, 2019, pp. 147–152. 4

[20] M. Young, Thermal imaging in the historic environment, 1st Edition, Historic Environment Scotland – Scottish Charity, 2015. 4

[21] C. A. Balaras, A. Argiriou, Infrared thermography for building diagnostics, Energy and buildings 34 (2) (2002) 171–183. 4

[22] M. Fox, D. Coley, S. Goodhew, P. De Wilde, Time-lapse thermography for building defect detection, Energy and Buildings 92 (2015) 95–106. 4

[23] G. Vijayaraghavan, M. Majumder, K. Ramachandran, Quantitative analysis of delaminations in grp pipes using thermal ndte technique., Journal of Advanced Research in Mechanical Engineering 1 (1). 4

[24] A. Ellenberg, A. Kontsos, F. Moon, I. Bartoli, Bridge deck delamination identification from unmanned aerial vehicle infrared imagery, Automation in Construction 72 (2016) 155–165. 4

[25] S. Longhi, D. Marzioni, E. Alidori, G. Di Buo, M. Prist, M. Grisostomi, M. Pirro, Solid waste management architecture using wireless sensor network technology, in: 2012 5th International Conference on New Technologies, Mobility and Security (NTMS), IEEE, 2012, pp. 1–5. 4, 19

[26] V. Ruiz, Á. Sánchez, J. F. Vélez, B. Raducanu, Automatic image-based waste classification, in: International Work-Conference on the Interplay Between Natural and Artificial Computation, Springer, 2019, pp. 422–431. 7, 13, 14

[27] A. Singh, P. Aggarwal, R. Arora, Iot based waste collection system using infrared sensors, in: 2016 5th International Conference on Reliability, Infocom Technologies and Optimization (Trends and Future Directions)(ICRITO), IEEE, 2016, pp. 505–509. 7, 13, 14

[28] J. Fraden, Handbook of modern sensors: Physics, Designs, and Applications 17 (2) (2003) 499–501. 7

[29] G. Brooker, Introduction to sensors for ranging and imaging, The Institution of Engineering and Technology, 2009. 7

[30] P. W. Kruse, et al., Uncooled thermal imaging: arrays, systems, and applications, Vol. 2003, SPIE press Bellingham, WA, 2001. 8

[31] A. Mehta, Introduction to the electromagnetic spectrum and spectroscopy, Analytical Chemistry), Pharmaxchange, Aug. 8

[32] Y. Abdelrahman, E. Velloso, T. Dingler, A. Schmidt, F. Vetere, Cognitive heat: exploring the usage of thermal imaging to unobtrusively estimate cognitive load, Proceedings of the ACM on Interactive, Mobile, Wearable and Ubiquitous Technologies 1 (3) (2017) 33. 8

[33] R. Gade, T. B. Moeslund, Thermal cameras and applications: a survey, Machine vision and applications 25 (1) (2014) 245–262. 9

[34] J. B. Mercer, E. F. J. Ring, Fever screening and infrared thermal imaging: concerns and guidelines, Thermology International 19 (3) (2009) 67–69. 11

[35] G. Sun, S. Abe, O. Takei, T. Matsui, A portable screening system for onboard entry screening at international airports using a microwave radar, reflective photo sensor and thermography, in: 2011 2nd International Conference on Instrumentation, Communications, Information Technology, and Biomedical Engineering, IEEE, 2011, pp. 107–110. 11

[36] M. Adam, E. Y. Ng, J. H. Tan, M. L. Heng, J. W. Tong, U. R. Acharya, Computer aided diagnosis of diabetic foot using infrared thermography: A review, Computers in biology and medicine 91 (2017) 326–336. 11

[37] H. Qi, N. A. Diakides, Thermal infrared imaging in early breast cancer detection-a survey of recent research, in: Proceedings of the 25th Annual International Conference of the IEEE Engineering in Medicine and Biology Society (IEEE Cat. No. 03CH37439), Vol. 2, IEEE, 2003, pp. 1109–1112. 11

[38] B. Harangi, T. Csordás, A. Hajdu, Detecting the excessive activation of the ciliaris muscle on thermal images, in: 2011 IEEE 9th International Symposium on Applied Machine Intelligence and Informatics (SAMI), IEEE, 2011, pp. 329–331. 11

[39] K. Kondo, N. Kakuta, T. Chinzei, Y. Nasu, T. Suzuki, T. Saito, A. Wagatsuma, H. Ishigaki, K. Mabuchi, Thermal rhythmography-topograms of the spectral analysis of fluctuations in skin temperature, in: 2001 Conference Proceedings of the 23rd Annual International Conference of the IEEE Engineering in Medicine and Biology Society, Vol. 3, IEEE, 2001, pp. 2812–2815. 11

[40] A. Mahmoud, A. El-Barkouky, H. Farag, J. Graham, A. Farag, A non-invasive method for measuring blood flow rate in superficial veins from a single thermal image, in: Proceedings of the IEEE Conference on Computer Vision and Pattern Recognition Workshops, 2013, pp. 354–359. 11

[41] M. K. Bhowmik, D. Bhattacharjee, M. Nasipuri, D. K. Basu, M. Kundu, Classification of polar-thermal eigenfaces using multilayer perceptron for human face recognition, in: 2008 IEEE Region 10 and the Third international Conference on Industrial and Information Systems, IEEE, 2008, pp. 1–6. 11

[42] B. A. Rajoub, R. Zwiggelaar, Thermal facial analysis for deception detection, IEEE transactions on information forensics and security 9 (6) (2014) 1015–1023. 11

[43] I. Pavlidis, Detection system and method using thermal image analysis, uS Patent 6,996,256 (Feb. 7 2006). 11

[44] J.-H. Hwang, S. Jun, S.-H. Kim, D. Cha, K. Jeon, J. Lee, Novel fire detection device for robotic fire fighting, in: ICCAS 2010, IEEE, 2010, pp. 96–100. 11

[45] B. C. Arrue, A. Ollero, J. M. De Dios, An intelligent system for false alarm reduction in infrared forest-fire detection, IEEE Intelligent Systems and Their Applications 15 (3) (2000) 64–73. 11

[46] J. Price, C. Maraviglia, W. Seisler, E. Williams, M. Pauli, System capabilities, requirements and design of the gdl gunfire detection and location system, in: 33rd Applied Imagery Pattern Recognition Workshop (AIPR'04), IEEE, 2004, pp. 257–262. 11

[47] A. Goodchild, J. Toy, Delivery by drone: An evaluation of unmanned aerial vehicle technology in reducing co2 emissions in the delivery service industry, Transportation Research Part D: Transport and Environment 61 (2018) 58–67. 12

[48] Y. M. Chen, L. Dong, J.-S. Oh, Real-time video relay for uav traffic surveillance systems through available communication networks, in: 2007 IEEE wireless communications and networking conference, IEEE, 2007, pp. 2608–2612. 12

[49] L. Apvrille, T. Tanzi, J.-L. Dugelay, Autonomous drones for assisting rescue services within the context of natural disasters, in: 2014 XXXIth URSI General Assembly and Scientific Symposium (URSI GASS), IEEE, 2014, pp. 1–4. 12

[50] L. Changchun, S. Li, W. Hai-bo, L. Tianjie, The research on unmanned aerial vehicle remote sensing and its applications, in: 2010 2nd International Conference on Advanced Computer Control, Vol. 2, IEEE, 2010, pp. 644–647. 12

[51] Y. Xiao, H. Zheng, W. Yu, Automatic crowd detection based on unmanned aerial vehicle thermal imagery, in: International Conference on Mechatronics and Intelligent Robotics, Springer, 2017, pp. 510–516. 12

[52] J. Casana, J. Kantner, A. Wiewel, J. Cothren, Archaeological aerial thermography: a case study at the chaco-era blue j community, new mexico, Journal of Archaeological Science 45 (2014) 207–219. 12

[53] A. Dhekne, M. Gowda, Y. Zhao, H. Hassanieh, R. R. Choudhury, Liquid: A wireless liquid identifier, in: Proceedings of the 16th Annual International Conference on Mobile Systems, Applications, and Services, ACM, 2018, pp. 442–454. 12

[54] S. Yue, D. Katabi, Liquid testing with your smartphone, in: Proceedings of the 17th Annual International Conference on Mobile Systems, Applications, and Services, ACM, 2019, pp. 275–286. 12, 13

[55] M. Wei, S. Huang, J. Wang, H. Li, H. Yang, S. Wang, The study of liquid surface waves with a smartphone camera and an image recognition algorithm, European Journal of Physics 36 (6) (2015) 065026. 12, 13

[56] H. Flores, A. Zuniga, N. H. Motlagh, M. Liyanage, M. Passananti, S. Tarkoma, M. Youssef, P. Nurmi, Penguin: aquatic plastic pollution sensing using auvs., in: DroNet@ MobiSys, 2020, pp. 5–1. 12, 13

[57] S. Klakegg, J. Goncalves, C. Luo, A. Visuri, A. Popov, N. van Berkel, Z. Sarsenbayeva, V. Kostakos, S. Hosio, S. Savage, et al., Assisted medication management in elderly care using miniaturised near-infrared spectroscopy, Proceedings of the ACM on Interactive, Mobile, Wearable and Ubiquitous Technologies 2 (2) (2018) 69. 13

[58] W. Jiang, et al., Probing sucrose contents in everyday drinks using miniaturized near-infrared spectroscopy scanners, Proceedings of the ACM on Interactive, Mobile, Wearable and Ubiquitous Technologies 3 (4) (2019) 1–25. 13

[59] Y. Cho, N. Bianchi-Berthouze, N. Marquardt, S. J. Julier, Deep thermal imaging: Proximate material type recognition in the wild through deep learning of spatial surface temperature patterns, in: Proceedings of the 2018 CHI Conference on Human Factors in Computing Systems, ACM, 2018, p. 2. 13

[60] H.-S. Yeo, J. Lee, A. Bianchi, D. Harris-Birtill, A. Quigley, Specam: sensing surface color and material with the front-facing camera of a mobile device, in: Proceedings of the 19th International Conference on Human-Computer Interaction with Mobile Devices and Services, ACM, 2017, p. 25. 13

[61] U. Ha, Y. Ma, Z. Zhong, T.-M. Hsu, F. Adib, Learning food quality and safety from wireless stickers., in: HotNets, 2018, pp. 106–112. 13

[62] D. Lin, P. Westfeld, H.-G. Maas, Shutter-less temperature-dependent correction for uncooled thermal camera under fast changing fpa temperature, The International Archives of Photogrammetry, Remote Sensing and Spatial Information Sciences 42 (2017) 619. 13

BIBLIOGRAPHY

[63] S. P. Gundupalli, S. Hait, A. Thakur, A review on automated sorting of source-separated municipal solid waste for recycling, Waste management 60 (2017) 56–74. 13

[64] D. Scott, A two-colour near-infrared sensor for sorting recycled plastic waste, Measurement Science and Technology 6 (2) (1995) 156. 13

[65] J. Huang, T. Pretz, Z. Bian, Intelligent solid waste processing using optical sensor based sorting technology, in: 2010 3rd international congress on image and signal processing, Vol. 4, IEEE, 2010, pp. 1657–1661. 13

[66] A. Picón, A. Bereciartua, J. Echazarra, O. Ghita, P. F. Whelan, P. M. Iriondo, Real-time hyperspectral processing for automatic nonferrous material sorting, Journal of Electronic Imaging 21 (1) (2012) 013018. 13

[67] S. Serranti, A. Gargiulo, G. Bonifazi, Characterization of post-consumer polyolefin wastes by hyperspectral imaging for quality control in recycling processes, Waste Management 31 (11) (2011) 2217–2227. 13

[68] S. P. Gundupalli, S. Hait, A. Thakur, Multi-material classification of dry recyclables from municipal solid waste based on thermal imaging, Waste management 70 (2017) 13–21. 13, 22

[69] S. P. Gundupalli, S. Hait, A. Thakur, Classification of metallic and non-metallic fractions of e-waste using thermal imaging-based technique, Process Safety and Environmental Protection 118 (2018) 32–39. 13

[70] R. A. Aral, Ş. R. Keskin, M. Kaya, M. Hacıömeroğlu, Classification of trashnet dataset based on deep learning models, in: 2018 IEEE International Conference on Big Data (Big Data), IEEE, 2018, pp. 2058–2062. 14

[71] J. Hopewell, R. Dvorak, E. Kosior, Plastics recycling: challenges and opportunities, Philosophical Transactions of the Royal Society B: Biological Sciences 364 (1526) (2009) 2115–2126. 19

[72] H. Lester, History and physical chemistry of hdpe, Plastics Pipe Institute. 20

[73] J. Puls, S. A. Wilson, D. Hölter, Degradation of cellulose acetate-based materials: a review, Journal of Polymers and the Environment 19 (1) (2011) 152–165. 20

[74] M. Forrest, Recycling and re-use of waste rubber, Smithers Rapra, 2014. 20

[75] M. Nuzaimah, S. Sapuan, R. Nadlene, M. Jawaid, Recycling of waste rubber as fillers: A review, in: IOP Conference Series: Materials Science and Engineering, Vol. 368, IOP Publishing, 2018, p. 012016. 20

[76] R. Siddique, Waste materials and by-products in concrete, Springer Science & Business Media, 2007. 20

[77] S. Mishra, R. N. Bharagava, N. More, A. Yadav, S. Zainith, S. Mani, P. Chowdhary, Heavy metal contamination: An alarming threat to environment and human health, in: Environmental biotechnology: For sustainable future, Springer, 2019, pp. 103–125. 21

[78] V. John, Introduction to engineering materials, Macmillan International Higher Education, 1992. 21

[79] Y. Pranolo, W. Zhang, C. Cheng, Recovery of metals from spent lithium-ion battery leach solutions with a mixed solvent extractant system, Hydrometallurgy 102 (1-4) (2010) 37–42. 21

[80] N. B. Horeh, S. Mousavi, S. Shojaosadati, Bioleaching of valuable metals from spent lithium-ion mobile phone batteries using aspergillus niger, Journal of Power Sources 320 (2016) 257–266. 21

[81] P. Schober, C. Boer, L. A. Schwarte, Correlation coefficients: appropriate use and interpretation, Anesthesia & Analgesia 126 (5) (2018) 1763–1768. 22

[82] T. Malmivirta, J. Hamberg, E. Lagerspetz, X. Li, E. Peltonen, H. Flores, P. Nurmi, Hot or not? robust and accurate continuous thermal imaging on flir cameras, in: IEEE International Conference on Pervasive Computing and Communications, IEEE, 2019, pp. 1–9. 27

[83] N. C. of Examiners for Engineering, Fundamentals of Engineering: Supplied-reference Handbook, Kaplan AEC Engineering, 2003. 28

[84] L. Breiman, Random forests, UC Berkeley TR567. 29

[85] R. Genuer, V. Michel, E. Eger, B. Thirion, Random forests based feature selection for decoding fmri data, in: Proceedings Compstat, Vol. 267, 2010, pp. 1–8. 29

[86] Y. Qi, Random forest for bioinformatics, in: Ensemble machine learning, Springer, 2012, pp. 307–323. 29

[87] L. Zhang, Z. Liu, T. Ren, D. Liu, Z. Ma, L. Tong, C. Zhang, T. Zhou, X. Zhang, S. Li, Identification of seed maize fields with high spatial resolution and multiple spectral remote sensing using random forest classifier, Remote Sensing 12 (3) (2020) 362. 29

[88] L. Breiman, Bagging predictors, Machine learning 24 (2) (1996) 123–140. 29

[89] M. Pal, Random forest classifier for remote sensing classification, International journal of remote sensing 26 (1) (2005) 217–222. 29

[90] J. S. Sartakhti, M. H. Zangooei, K. Mozafari, Hepatitis disease diagnosis using a novel hybrid method based on support vector machine and simulated annealing (svm-sa), Computer methods and programs in biomedicine 108 (2) (2012) 570–579. 31

[91] L. Hu, J. Cui, Digital image recognition based on fractional-order-pca-svm coupling algorithm, Measurement 145 (2019) 150–159. 31

[92] Z.-Q. Wang, X. Sun, D.-X. Zhang, X. Li, An optimal svm-based text classification algorithm, in: 2006 International Conference on Machine Learning and Cybernetics, IEEE, 2006, pp. 1378–1381. 31

[93] R. Schalkoff, Syntactic pattern recognition (syntpr) overview, Pattern Recognition: Statistical, Structural and Neural Approaces (1992) 127–150. 31

[94] Z. Obermeyer, J. K. Samra, S. Mullainathan, Individual differences in normal body temperature: longitudinal big data analysis of patient records, Bmj 359. 33, 36, 51

[95] Z. Sarsenbayeva, et al., Sensing cold-induced situational impairments in mobile interaction using battery temperature, Proceedings of the ACM on Interactive, Mobile, Wearable and Ubiquitous Technologies 1 (3) (2017) 1–9. 40

[96] E. Ring, K. Ammer, Infrared thermal imaging in medicine, Physiological measurement 33 (3) (2012) R33. 47

[97] H. Emenike, F. Dar, M. Liyanage, R. Sharma, A. Zuniga, M. Hoque, M. Radeta, P. Nurmi, H. Flores, Sensing residual dissipation of human-emitted thermal radiation, Pervasive Computing and Communications 1 (2021) 1–8. 56

9

Appendix

Table 9.1: Test model result

Results for 100 repetitions, using the full dataset. 80% train, 25% test, 5% validation								
			Test					
Predicted	Features	Statistic	Random Forest	SVM	AdaBoost	MLPC	**AVERAGE**	**MEDIAN**
Material	(vector)	mean	0.59	0.588	0.565	0.585	0.582	0.587
		std	0.032	0.038	0.04	0.039	0.037	0.038
		median	0.588	0.588	0.561	0.588	0.581	0.588
		max	0.658	0.667	0.649	0.702	0.669	0.662
	(vector, context)	mean	0.589	0.569	0.565	0.579	0.575	0.574
		std	0.04	0.036	0.04	0.038	0.039	0.039
		median	0.592	0.566	0.561	0.579	0.575	0.572
		max	0.684	0.64	0.649	0.702	0.669	0.667
	(vector,gender)	mean	0.592	0.56	0.564	0.578	0.573	0.571
		std	0.035	0.034	0.04	0.04	0.037	0.038
		median	0.588	0.561	0.561	0.579	0.572	0.57
		max	0.667	0.64	0.649	0.675	0.658	0.658
	(vector,gender,context)	mean	0.586	0.54	0.564	0.561	0.563	0.562
		std	0.035	0.036	0.04	0.041	0.038	0.038
		median	0.588	0.535	0.561	0.561	0.561	0.561
		max	0.675	0.623	0.649	0.649	0.649	0.649
Context	(material, vector)	mean	0.509	0.523	0.512	0.537	0.52	0.518
		std	0.044	0.042	0.04	0.045	0.043	0.043
		median	0.509	0.526	0.509	0.539	0.521	0.518
		max	0.623	0.64	0.596	0.667	0.632	0.632
Gender	(material, vector)	mean	0.616	0.618	0.651	0.609	0.623	0.617
		std	0.034	0.025	0.019	0.036	0.028	0.03
		median	0.614	0.623	0.649	0.605	0.623	0.618
		max	0.693	0.684	0.693	0.702	0.693	0.693

Table 9.2: Validation of test model result

		Validation					
Predicted	Features	Random Forest	SVM	AdaBoost	MLPC	**AVERAGE**	**MEDIAN**
Material	(vector)	0.604	0.608	0.588	0.601	0.6	0.602
		0.119	0.092	0.096	0.109	0.104	0.103
		0.591	0.591	0.591	0.591	0.591	0.591
		0.909	0.773	0.818	0.818	0.83	0.818
	(vector, context)	0.599	0.598	0.588	0.6	0.596	0.598
		0.112	0.093	0.096	0.099	0.1	0.097
		0.636	0.591	0.591	0.591	0.602	0.591
		0.909	0.773	0.818	0.818	0.83	0.818
	(vector,gender)	0.605	0.575	0.584	0.599	0.591	0.591
		0.113	0.104	0.094	0.094	0.101	0.099
		0.614	0.591	0.591	0.591	0.597	0.591
		0.909	0.864	0.818	0.818	0.852	0.841
	(vector,gender,context)	0.599	0.566	0.584	0.584	0.583	0.584
		0.104	0.101	0.093	0.097	0.099	0.099
		0.591	0.545	0.591	0.591	0.58	0.591
		0.864	0.818	0.818	0.818	0.83	0.818
Context	(material, vector)	0.52	0.524	0.524	0.529	0.524	0.524
		0.101	0.101	0.097	0.102	0.1	0.101
		0.5	0.5	0.545	0.545	0.523	0.523
		0.773	0.818	0.773	0.727	0.773	0.773
Gender	(material, vector)	0.601	0.617	0.64	0.588	0.612	0.609
		0.077	0.07	0.047	0.1	0.073	0.073
		0.591	0.636	0.636	0.591	0.614	0.614
		0.773	0.773	0.773	0.818	0.784	0.773

Table 9.3: Cross validation of test model result

		Cross-validation					
Predicted	Features	Random Forest	SVM	AdaBoost	MLPC	**AVERAGE**	**MEDIAN**
Material	(vector)	0.599	0.597	0.564	0.608	0.592	0.598
		0	0	0	0	0	0
		0.599	0.597	0.564	0.608	0.592	0.598
		0.599	0.597	0.564	0.608	0.592	0.598
	(vector, context)	0.588	0.593	0.564	0.56	0.576	0.576
		0	0	0	0	0	0
		0.588	0.593	0.564	0.56	0.576	0.576
		0.588	0.593	0.564	0.56	0.576	0.576
	(vector,gender)	0.586	0.589	0.569	0.586	0.582	0.586
		0	0	0	0	0	0
		0.586	0.589	0.569	0.586	0.582	0.586
		0.586	0.589	0.569	0.586	0.582	0.586
	(vector,gender,context)	0.595	0.575	0.569	0.589	0.582	0.582
		0	0	0	0	0	0
		0.595	0.575	0.569	0.589	0.582	0.582
		0.595	0.575	0.569	0.589	0.582	0.582
Context	(material, vector)	0.558	0.538	0.518	0.542	0.539	0.54
		0	0	0	0	0	0
		0.558	0.538	0.518	0.542	0.539	0.54
		0.558	0.538	0.518	0.542	0.539	0.54
Gender	(material, vector)	0.6	0.628	0.633	0.648	0.627	0.631
		0	0	0	0	0	0
		0.6	0.628	0.633	0.648	0.627	0.631
		0.6	0.628	0.633	0.648	0.627	0.631

9.1 Licence

Non-exclusive licence to reproduce thesis and make thesis public
I, Hilary Somtochukwu Emenike,

1. herewith grant the University of Tartu a free permit (non-exclusive licence) to reproduce, for the purpose of preservation, including for adding to the DSpace digital archives until the expiry of the term of copyright,

   Exploiting Human-emitted Thermal Radiation,

   supervised by Huber Flores.

2. I grant the University of Tartu a permit to make the work specified in p. 1 available to the public via the web environment of the University of Tartu, including via the DSpace digital archives, under the Creative Commons licence CC BY NC ND 3.0, which allows, by giving appropriate credit to the author, to reproduce, distribute the work and communicate it to the public, and prohibits the creation of derivative works and any commercial use of the work until the expiry of the term of copyright.

3. I am aware of the fact that the author retains the rights specified in p. 1 and 2.

4. I certify that granting the non-exclusive licence does not infringe other persons' intellectual property rights or rights arising from the personal data protection legislation.

Hilary Somtochukwu Emenike
14/1/2020